

ANL-HEP-PR-95-19
UF-IFT-HEP-95-21

GAUGE THEORY HIGH-ENERGY BEHAVIOR FROM J-PLANE UNITARITY *

Claudio Corianò^{a,b†} and Alan. R. White^{a#}

^aHigh Energy Physics Division
Argonne National Laboratory
9700 South Cass, IL 60439, USA.

^bInstitute for Fundamental Theory
Department of Physics
University of Florida at Gainesville, FL 32611, USA

Abstract

In a non-abelian gauge theory the t -channel multiparticle unitarity equations continued in the complex j -plane can be systematically expanded around $j = 1$. The combination of Ward identity constraints with unitarity is sufficient to produce directly many results obtained by Regge limit leading-log and next-to-leading log momentum space calculations. The $O(g^2)$ BFKL kernel is completely determined. $O(g^4)$ contributions to the kernel are also determined, including the leading contribution of a new partial-wave amplitude - previously identified as a separate forward component with a holomorphically factorizable spectrum. For this amplitude the only scale ambiguity is the overall normalization and it is anticipated to be a new conformally invariant kernel. The results suggest that all conformally invariant reggeon interactions are determined by t -channel unitarity.

*Work supported by the U.S. Department of Energy, Division of High Energy Physics, Contracts W-31-109-ENG-38 and DEFG05-86-ER-40272

† coriano@phys.ufl.edu #arw@hep.anl.gov

1. INTRODUCTION

The Regge limit of *QCD* is a challenging theoretical problem which will surely continue to be addressed for some time to come - particularly if the solution is fundamental to obtaining a full solution of the theory[1, 2]. The inter-relation of the Regge limit with the small-x behavior of structure functions and other new “hard diffractive” experimental phenomena recently observed at HERA and the Tevatron Collider has been the subject of much recent investigation. Indeed, the leading-log BFKL equation[3], originally derived in the Regge limit, has now been applied extensively in the study of parton distributions at small-x. A further factor in stimulating recent theoretical activity has been the development of new techniques which offer the hope of greater insight into the physics involved. In particular, a two-dimensional effective theory[4, 5] has been developed which reproduces the leading order perturbative calculations[3, 6] and which it is hoped can be used as input to some form of “*s*-channel” unitarisation scheme.

In this paper our emphasis will be on the development of new techniques for the exploitation of “*t*-channel” unitarity, rather than *s*-channel unitarity, to determine corrections to leading-order results. The kernel of the BFKL equation can be viewed as a 2-2 reggeon interaction and in [7] we have suggested that the non-leading, $O(g^4)$, “scale-invariant” part of this kernel can be derived directly by a “reggeon diagram technique”. This technique assumes that reggeized gluon interactions can be constructed from reggeon diagrams in which the gluon couples via a “nonsense-zero” triple vertex. Effectively, all contributions of gluons to reggeon interactions are assumed to be traceable back to *t*-channel reggeized gluon exchanges. The justification for the use of reggeon diagrams in this manner is that constraints of multiparticle *t*-channel unitarity are, at least partially, satisfied. However, it is easy to criticize the assumptions made and our aim in this paper is to give a more fundamental derivation of the results directly from *t*-channel unitarity continued in the complex angular momentum plane (the *j*-plane).

Our analysis is based entirely on combining unitarity and gauge invariance with a weak-coupling expansion of the theory around $j = 1$. We avoid momentum space calculations altogether. It might be thought that some calculations are needed to input the defining lagrangian. In fact, as we already pointed out in [7], gauge invariance can be input via the Ward identity requirement that reggeon amplitudes vanish at zero transverse momentum and the gauge group can be inserted via the

group structure of the lowest-order reggeon interaction (i.e. the triple Regge vertex). We will obtain both the reggeization and explicit higher-order results using only these ingredients as defining elements of the theory. Consequently, we make at least partial progress towards the direct perturbative construction of “Yang-Mills reggeon theories” envisaged in [7].

Perturbatively expanding the unitarity equations around $j = 1$ should be equivalent to expanding in powers of leading, next-to-leading etc., Regge limit logarithms. This equivalence, at first sight, should enable us to compare our j -plane analysis directly with momentum space calculations. However, the unitarity analysis gives only the t -channel discontinuities responsible for the leading infra-red behavior of amplitudes. Therefore our formalism gives reliable results only at small transverse momentum. Small has, of course, to be defined in terms of some scale which breaks transverse momentum scale-invariance and we will not discuss this. However, we expect that the infra-red analysis will be sufficient to find all conformally invariant reggeon interactions and our results are consistent with this expectation. (We should note that it is not yet clear to what extent the momentum space evaluation[8] of non-leading log amplitudes avoids ambiguities associated with the introduction of scales, particularly that associated with renormalization and the large momentum evolution of the coupling constant.)

A major issue is that the reggeon diagram method used in [7] implicitly assumes a reduction to transverse momentum integrals which a-priori is not justified and which next-to-leading order s -channel calculations apparently do not give[5]. We will show that this reduction is always justified when only “nonsense” t -channel gluon states are involved in producing a reggeon interaction. (In general, “nonsense states” have less angular momentum than helicity - as a result of analytic continuation in j . Note also that in our analysis the two-dimensional “transverse momentum” variables, that we refer to throughout, are the t -channel timelike counterpart of s -channel transverse momenta.) We will show that the BFKL kernel actually arises entirely from nonsense states, as does that part of the $O(g^4)$ kernel that we have separated in [9] as having distinct infra-red finiteness and holomorphic factorization properties. Indeed we will show that this $O(g^4)$ contribution is actually *a new partial-wave amplitude which appears for the first time at this order*. Correspondingly the only scale ambiguity is the overall normalization. In a companion paper[10] we construct what we conjecture to be the non-forward conformally invariant form of this amplitude.

The complete $O(g^4)$ kernel that we gave in [7] can not be unambiguously

derived from nonsense contributions. Even though we expect this kernel to be an infra-red “scale-invariant” approximation to the complete kernel. We will make very little reference to scale-dependent contributions. Note, however, that in a recent paper Kisrichner[11] has discussed how the $O(g^4)$ kernel can arise as an approximation when the leading-log s -channel multi-Regge effective lagrangian is used. A number of s -channel contributions have to be combined to reproduce the simplicity of the t -channel reggeon diagram results.

Even if the program[8] to calculate the next-to-leading order BFKL kernel can be completed in momentum space, it seems inevitable that study of the high-energy behavior of QCD will eventually move, in large part, to the complex j -plane. The direct calculation of logarithms is extremely complicated compared to the simplicity of the results when expressed in j -plane language. (To realize the economy of language, one has only to compare the simple Regge pole formula for electron exchange that is the outcome, with the 240 pages of the Physical Review used[12] by McCoy and Wu to calculate to twelfth order in QED.) All of t -channel unitarity, particularly reggeon unitarity, can be simply expressed in the j -plane. The structure of multiparticle partial-wave amplitudes is also only apparent in this language. In particular the new $O(g^4)$ amplitude we discuss would be very hard to isolate in s -channel calculations. In general it seems likely that the complexity of an s -channel effective lagrangian formalism[5] will obscure many of the t -channel simplifications. If the problem of higher-order corrections can be transferred to the j -plane, as we will partially succeed in doing, then it is possible that significantly more progress can be made. To put our efforts in context we give a very brief historical review of the development of t -channel unitarity as a tool to study both abstract Regge theory and the Regge behavior of gauge theories in particular.

Reggeon diagrams, or Reggeon Field Theory (RFT) as the formalism came to be called, originally arose from the “hybrid Feynman diagram” formalism of Gribov[13]. Part of Gribov’s motivation for developing the diagrammatic formalism was to provide an interpretation of the abstract results of Gribov, Pomeranchuk and Ter-Martirosyan (GPT) obtained from multiparticle t -channel unitarity continued in the complex j -plane[14]. The GPT work was in turn a response to Mandelstam’s work[15] showing that t -channel unitarity could be reliably used to calculate the high-energy behaviour of Feynman graphs giving Regge cut behaviour, whereas s -channel unitarity was unreliable. (As remains true in current gauge theory calculations, there are many cancellations amongst s -channel states, while t -channel states give easily distinguished contributions.) The GPT results gave discontinuity formulae for the

angular momentum plane branch points (Regge cuts) due to general multiple Regge pole exchange. The relationship of the reggeon diagrams formulated by Gribov to the angular momentum plane unitarity formulae was analogous to that of conventional Feynman diagrams to normal momentum space unitarity. However, there were various analytic continuation and summation ambiguities in the GPT formulae and, at the time, it seemed that explicit diagrammatic calculations of the kind developed by Gribov would be the only way to resolve such ambiguities. The direct diagrammatic approach also seemed simpler than the complicated GPT formalism.

Subsequently major progress was made in understanding the analyticity properties of multiparticle amplitudes[16, 17, 18]. Asymptotic dispersion relations were derived and provided the basis for a comprehensive development of abstract multiparticle complex angular momentum theory. All the ambiguities of the GPT work were resolved and the resulting discontinuity formulae, or *reggeon unitarity equations* were established. The most immediate application was to provide an underlying framework for the study of Pomeron RFT. It was understood that, given the lowest order reggeon interactions, the reggeon unitarity equations determine the form of the general reggeon diagrams of a complete RFT. (The generality of the circumstances under which the very attractive *Critical Pomeron* solution[19] of RFT could appear as the true asymptotic behavior of the strong interaction became particularly clear.)

The reggeization of the gluon, in a gauge theory, was actually first obtained[20] by j -plane analysis of two-particle t -channel unitarity. Only later was this confirmed in leading-log momentum-space calculations. Once gluon reggeization is established, the reggeon unitarity equations determine that the non-leading logs must reduce to an effective two-dimensional theory which can be described in terms of reggeon diagrams. Indeed, it has already been demonstrated[21] that in Yang-Mills theories leading and next-to-leading logarithms are very compactly described by reggeon diagrams - providing the most direct way to derive the BFKL equation. We expect that a full set of such diagrams should describe the leading power *plus all logarithms* obtained from perturbation theory. In principle new Regge trajectories may emerge in higher-orders, the symmetric octet trajectory found by Bartels and Wüsthoff[22] being an example. However, although we will not elaborate on our reasons, we do not expect this to be an extended phenomenon.

At first sight only the general form of the phase-space in reggeon diagrams is determined by reggeon unitarity and so it would be anticipated that reggeon interactions should be extracted from momentum space calculations as in [21]. A related point is that, although reggeization was derived using two-particle unitarity[20], it

was necessary to first calculate the lowest-order nonsense amplitudes via momentum space. Effectively, our purpose in this paper is to show that, when gauge invariance and the gauge group are input as we have discussed, reggeon unitarity can also be used to determine reggeon interactions in gauge theories. It will be essential to expand the concept of reggeon unitarity to include the contribution of “right-signature” reggeon nonsense states. The key to this will be, as we have already emphasized, the weak-coupling expansion around $j = 1$ - which is a “nonsense point” in a reggeized vector theory. Since the reggeons of a gauge theory are odd-signature reggeized gluons, the reggeon propagators and interactions appearing in the diagrams contain particle poles in addition to Regge poles. The particle poles give “right-signature nonsense state thresholds” in t (in contrast to the Regge cuts which can be described as “wrong-signature nonsense state thresholds” in j). It is by determining the discontinuity across the t -thresholds directly from unitarity that we actually determine the reggeon interactions.

We should note that the particle poles in reggeon diagrams also produce infra-red divergences and as a consequence, the diagrams are all infra-red divergent. We have discussed the dynamical implications of these divergences, for the “non-perturbative” solution of the theory, at length in [1] and, of course, the divergences cancel in the physical kernels appearing in the BFKL equation. In this paper we will regard the divergences as a purely technical problem that we will ignore in deriving explicit formulae. The massless theory is particularly simple and our central purpose is to show how far we can go in this case.

Since the formalism we will use is very unfamiliar to most physicists we will spend a considerable time just introducing concepts and language. We begin in Section 2 by providing a very elementary outline of our analysis. In Section 3 we cover various preliminary topics. We formulate the leading-order BFKL equation in reggeon language, discuss the origin of reggeon Ward identity constraints and introduce a diagrammatic notation for color factors. Section 4 contains a review of nonsense states, transverse momentum diagrams and Regge cut discontinuity formulae, as well as a rederivation of the reggeization of the gluon in our formalism. In Section 5 we rederive the BFKL kernel before proceeding, in Section 6, to the derivation of $O(g^4)$ reggeon interactions. The crucial result is the demonstration that amongst the $O(g^4)$ interactions is a leading-order contribution to a new partial-wave amplitude. Section 7 contains some brief conclusions and comments.

2. OUTLINE OF THE ANALYSIS

In this Section we outline the arguments developed at length in the following Sections. We will avoid precise definitions in the interests of presenting a simple overview.

We consider a reggeon theory containing a vector particle (which is, of course, the gluon) lying on a Regge trajectory

$$j \equiv 1 + \omega = \alpha(t) = 1 + \Delta(q^2), \quad (2.1)$$

which, if the particle is massless, satisfies

$$\Delta(0) = \alpha(0) - 1 = 0 \quad (2.2)$$

In the j -plane there is a Regge pole - produced by a “reggeon propagator” which we represent diagrammatically as in Fig. 2.1

$$\overbrace{\hspace{1cm}} = \frac{1}{\omega + \Delta(q^2)}$$

Fig. 2.1 The Reggeon Propagator

As we review in Section 4, it follows from t -channel unitarity that there will also be Regge cuts, or “thresholds”, in the j -plane, arising from the exchange of any number of reggeons. The N -reggeon cut arises from phase-space integration of the N -reggeon propagator which, in the language we develop, is simply a “nonsense pole”. The phase-space is an integral over the transverse momenta of the reggeons. (As we noted in the Introduction, these are actually time-like two dimensional momenta in our analysis). For example, the two-reggeon cut arises from

$$\int \frac{d^2 k_1}{k_1^2} \frac{d^2 k_2}{k_2^2} \delta^2(q - k_1 - k_2) \Gamma_2 \quad (2.3)$$

where Γ_2 is the two-reggeon propagator represented in Fig. 2.2.

$$\begin{array}{c} \mathbf{k}_1 \\ \mathbf{k}_2 \end{array} \overbrace{\hspace{1cm}} \equiv \prod_2 (\omega, \mathbf{k}_1, \mathbf{k}_2) = \frac{1}{\omega + \Delta(\mathbf{k}_1^2) + \Delta(\mathbf{k}_2^2)}$$

Fig. 2.2 The two reggeon propagator

A complete set of reggeon diagrams satisfying reggeon unitarity is generated by introducing a general set of reggeon interaction vertices coupling the reggeon propagators. The lowest-order 2-2 reggeon vertex is the BFKL kernel.

We construct both the reggeon trajectory function and the reggeon interaction vertices from the following ingredients.

- [2A] Gauge invariance is input via the Ward identity constraint that all reggeon interaction vertices vanish when any reggeon transverse momentum goes to zero.
- [2B] The “nonsense” zero/pole structure required by general analyticity properties is imposed, in addition to Ward Identity zeroes.
- [2C] The group structure is input via the triple reggeon vertex, which couples (a nonsense state of) two reggeons to a single reggeon carrying transverse momentum q , i.e.

$$\text{Diagram: a wavy line meeting a vertical line, which then splits into two horizontal lines.} = \mathbf{r}_{ijk}(q^2) = g \mathbf{c}_{ijk} q^2$$

g is a dimensionless coupling, the c_{ijk} are the group structure constants (of $SU(N)$), and the factor of q^2 is determined by [2A] and [2B].

- [2D] t -channel unitarity is used to determine both j -plane Regge cut discontinuities and particle threshold discontinuities due to “nonsense” states.
- [2E] The j -plane and t -plane discontinuity formulae are expanded simultaneously around $j = 1$ ($\omega = 0$) and in powers of g^2 .

The most important ingredient is [2D] - the direct computation of t -channel nonsense state discontinuities. While unitarity determines that reggeon states produce transverse momentum integrals, we will see that for the particle discontinuities to be written as transverse momentum integrals it is necessary that only nonsense states are involved. When this is the case, it is straightforward to simultaneously expand the discontinuity equations in inverse powers of ω and powers of g^2 to determine interactions etc. in terms of transverse momentum integrals. For example, the $O(g^2)$ contribution to the trajectory function $\Delta(q^2)$ is obtained from the two-particle discontinuity of the reggeon propagator illustrated in Fig. 2.3

$$\sim \circlearrowleft \sim \circlearrowright - \sim \circlearrowleft \circlearrowright \sim \circlearrowleft = \sim \circlearrowleft \circlearrowright \circlearrowleft \circlearrowright \sim \circlearrowleft$$

Fig. 2.3 The two particle discontinuity of the reggeon propagator

Inserting the structure of the leading-order amplitudes implied by [2A], [2B] and [2C] we obtain

$$\frac{1}{\omega - \Delta(q^2)} - \frac{1}{\omega - \Delta^*(q^2)} = \frac{g^2 \sum_{j,k}^N c_{ijk} c_{ijk} q^2 \delta_{q^2} \{J_1(q^2)\}}{(\omega - \Delta(q^2))(\omega - \Delta^*(q^2))} \quad (2.4)$$

where $\delta_{q^2} \{ \}$ denotes the discontinuity in q^2 and

$$J_1(q^2) = \frac{1}{16\pi^3} \int \frac{d^2 k}{k^2 (k - q)^2} \quad (2.5)$$

From (2.4) we obtain

$$\Delta(q^2) = g^2 N q^2 J_1(q^2) + O(g^4) \quad (2.6)$$

$O(g^4)$ contributions may come from both the two and three-particle states.

We obtain the 2-2 reggeon interaction, i.e. the BFKL kernel, from the nonsense-state discontinuities of the two reggeon propagator Green function illustrated in Fig. 2.4.

$$\sim \circlearrowleft \circlearrowright \sim \circlearrowleft \circlearrowright - \sim \circlearrowleft \circlearrowright \sim \circlearrowleft \circlearrowright = \sim \circlearrowleft \circlearrowright \circlearrowleft \circlearrowright \sim \circlearrowleft \circlearrowright + \sim \circlearrowleft \circlearrowright \circlearrowleft \circlearrowright \sim \circlearrowleft \circlearrowright + \sim \circlearrowleft \circlearrowright \circlearrowleft \circlearrowright \sim \circlearrowleft \circlearrowright + \dots$$

Fig. 2.4 Nonsense state discontinuities of the two reggeon propagator Green function

The $O(g^2)$ kernel is derived, as $q^2 \rightarrow 0$, from the three-particle nonsense state. The contributions to the $O(g^4)$ kernel that we derive will be from the four-particle state. It will be an important part of our analysis to determine under what kinematic conditions the t -channel discontinuities involved are entirely due to nonsense states. We will impose not only $q^2 \rightarrow 0$ but also limit the individual transverse momenta of the reggeons involved.

3. THE $O(g^2)$ KERNEL, REGGEON LANGUAGE, WARD IDENTITIES AND GROUP FACTORS

Currently the most familiar application of the BFKL equation is to the evolution of parton distributions at small- x . We begin by recasting this equation in the reggeon diagram language in which it was originally derived in order to compare with our results in later Sections.

3.1 The BFKL Equation as a Reggeon Bethe-Salpeter Equation

If $F(x, k^2)$ is a parton distribution then the BFKL equation is

$$\frac{\partial}{\partial(\ln 1/x)} F(x, k^2) = \tilde{F}(x, k^2) + \frac{1}{16\pi^3} \int \frac{d^2 k'}{(k')^4} K(k, k') F(x, (k')^2) \quad (3.1)$$

where, if $SU(N)$ is the gauge group, $K(k, k')$ is given by

$$(Ng^2)^{-1} K(k, q) = \left(k^4 k'^2 J_1(k^2) \delta^2(k - k') - \frac{2k^2 k'^2}{(k - k')^2} \right) \quad (3.2)$$

To introduce reggeon language we rewrite the equation as a “reggeon Bethe-Salpeter equation” by, in effect, working backwards historically. We first extend (3.1) to the non-forward direction, then transform to ω - space (where ω is conjugate to $\ln \frac{1}{x}$), giving

$$\omega F(\omega, k, q - k) = \tilde{F} + \frac{1}{16\pi^3} \int \frac{d^2 k'}{(k')^2 (k' - q)^2} K(k, k', q) F(\omega, k', q - k') \quad (3.3)$$

where $K(k, k', q) = K_{2,2}^{(2)}(k, q - k, k', q - k')$ is now the full “non-forward” Lipatov kernel and contains three kinematic forms, i.e.

$$\begin{aligned} \frac{2}{Ng^2} K_{2,2}^{(2)}(k_1, k_2, k_3, k_4) &= (2\pi)^3 k_1^2 J_1(k_1^2) k_2^2 \left(k_3^2 \delta^2(k_2 - k_4) + k_4^2 \delta^2(k_2 - k_3) \right) \\ &\quad - \frac{k_1^2 k_4^2 + k_2^2 k_3^2}{(k_1 - k_3)^2} - (k_1 + k_2)^2 \\ &\equiv K_1 + K_2 + K_3 . \end{aligned} \quad (3.4)$$

Using a simple notation for transverse momentum diagrams i.e. using the components illustrated in Fig. 3.1.



Fig. 3.1 (a) vertices and (b) intermediate states in transverse momentum.

the rules for writing amplitudes corresponding to the diagrams are the following

- For each vertex, illustrated in Fig. 3.1(a), we write a factor

$$16\pi^3\delta^2(\sum k_i - \sum k'_i)(\sum k_i)^2$$

- For each intermediate state, illustrated in Fig. 3.1(b), we write a factor

$$(16\pi^3)^{-n} \int d^2 k_1 \dots d^2 k_n / k_1^2 \dots k_n^2$$

Dimensionless kernels are defined by a hat

$$\hat{K}_{2,2}^{(2)}(k_1, k_2, k_3, k_4) = 16\pi^3 \delta^2(k_1 + k_2 - k_3 - k_4) K_{2,2}^{(2)}(k_1, k_2, k_3, k_4)$$

The kernels so defined are formally scale-invariant (even though potentially infra-red divergent). The diagrammatic representation of $\hat{K}_{2,2}^{(2)}$, the non forward BFKL kernel, is then as in Fig. 3.2.

$$\sum \left(- \text{---} \text{---} + 2 \text{---} \text{---} - \text{---} \text{---} \right)$$

Fig. 3.2 Diagrammatic representation of $\hat{K}_{2,2}^{(2)}$

The summation sign again implies a sum over combined permutations of the initial and final momenta.

We introduce a two-reggeon propagator which corresponds to Fig. 2.2 with $\Delta(k^2)$ given by (2.6), i.e. we write

$$\Gamma_2(\omega, k_1, k_2) = [\omega - g^2 k_1^2 J_1(k_1^2) - g^2 J_1(k_2^2)]^{-1}, \quad (3.5)$$

moving the K_1 term to the left side of (3.3) and writing $G = \Gamma_2^{-1}F$ gives

$$G(\omega, k, q - k) = \tilde{G} + \frac{1}{(2\pi)^3} \int \frac{d^2 k'}{(k')^2 (k' - q)^2} \Gamma_2(\omega, k', q - k') \tilde{K}(k, k', q) G(\omega, k', q - k') \quad (3.6)$$

where now

$$\tilde{K}(k, k', q) = K_2 + K_3 = \frac{k_1^2 k_4^2 + k_2^2 k_3^2}{(k_1 - k_3)^2} - (k_1 + k_2)^2 \quad (3.7)$$

can be directly interpreted as a 2-2 reggeon interaction. That this interaction is singular is what makes it, at first sight, both difficult to anticipate and to generalize.

Note that if we take $\tilde{G} = \tilde{K}(k'', k, q)$ we obtain from (3.6) a full reggeon-reggeon scattering amplitude $\mathcal{G}(\omega, q, k'', k)$ which satisfies reggeon unitarity. That is, the Reggeon propagator in (3.6) produces a two-reggeon branch-cut in the ω -plane whose discontinuity is given by

$$\begin{aligned} \mathcal{G}(\omega^+, q, k'', k) - \mathcal{G}(\omega^-, q, k'', k) &= \frac{i}{(2\pi)^2} \int \frac{d^2 k'}{(k')^2 (k' - q)^2} \\ &\quad \delta[\omega - g^2 k'^2 J_1(k'^2) - g^2 (k' - q)^2 J_1((k' - q)^2)] \mathcal{G}(\omega^+, q, k'', k') \mathcal{G}(\omega^-, q, k', k) \end{aligned} \quad (3.8)$$

We can represent (3.8) diagrammatically as in Fig. 3.3.



Fig. 3.3 Reggeon Unitarity for a Reggeon-Reggeon Scattering Amplitude.

We shall also need the more general discontinuity formula which follows from (3.6) for a “particle-reggeon” scattering amplitude $G(\omega, k, q - k)$ defined with a general \tilde{G} i.e.

$$\begin{aligned} G(\omega^+, q, k) - G(\omega^+, q, k) &= \frac{i}{(2\pi)^2} \int \frac{d^2 k'}{(k')^2 (k' - q)^2} \\ &\quad \delta[\omega - g^2 k'^2 J_1(k'^2) - g^2 (k' - q)^2 J_1((k' - q)^2)] \mathcal{G}(\omega^+, q, k') \mathcal{G}(\omega^-, q, k', k) \end{aligned} \quad (3.9)$$

This is illustrated in Fig. 3.4.



Fig. 3.4 Reggeon Unitarity for a Particle-Reggeon Scattering Amplitude.

We emphasize that both (3.8) and (3.9) hold independently of the form of the reggeon interaction $\tilde{K}(k, k', q)$.

If we introduce a Regge slope α' as a regularising parameter and replace (3.5) by

$$\Gamma_2(\omega, k_1, k_2) = [\omega - \alpha' k_1^2 - \alpha' k_2^2]^{-1} \quad (3.10)$$

then (3.6) with K replacing \tilde{K} , also reduces to (3.3) in the limit $\alpha' \rightarrow 0$. In this way we can also interpret (3.3) directly as a reggeon equation in which the interaction (the full $K_{2,2}^{(2)}$) then has two vital properties

- It contains singularities (poles) but satisfies the “Ward Identity constraint”

$$K_{2,2}^{(2)}(k_1, k_2, k_3, k_4) \rightarrow 0, k_i \rightarrow 0, i = 1, \dots, 4 \quad (3.11)$$

- It is infra-red finite as an integral kernel i.e.

$$\int \frac{d^2 k_1}{k_1^2} \frac{d^2 k_2}{k_2^2} \delta^2(q - k_1 - k_2) K_{2,2}^{(2)}(k_1, k_2, k_3, k_4) \quad \text{is finite} \quad (3.12)$$

As we pointed out in [7], the two properties (3.11) and (3.12) determine the relative magnitude of the three kinematic forms K_1 , K_2 , and K_3 - assuming their existence can be derived from a general Regge theory argument. We will, of course, provide such an argument in the following Sections. However, while we will invoke the Ward identity constraint to determine the relative magnitude of K_2 and K_3 , we will show how the relative coefficients for K_1 and K_2 can be determined so that infra-red finiteness can be derived from unitarity. As we have stated several times already, and now discuss in more detail, the vanishing of reggeon amplitudes at zero transverse momentum is our input of gauge invariance into our analysis.

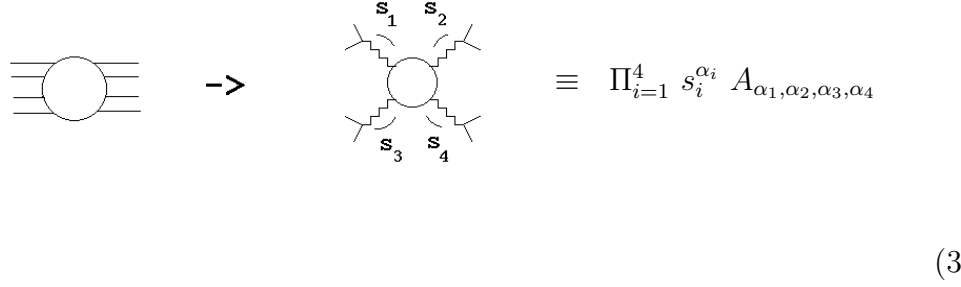
3.2 Gauge Invariance and Reggeon Ward Identities

As we briefly outlined in [7], imposing the vanishing of reggeon amplitudes at zero transverse momentum is directly equivalent to imposing the defining Ward

identities of the theory[23]. We now expand on this point. In this paper we will always define reggeon amplitudes as residues of multiple Regge poles in multiparticle partial-wave amplitudes, i.e. we write

$$a_{j_1, j_2, j_3, j_4, \dots} \xrightarrow{j_i \rightarrow \alpha_i, i=1, \dots, 4} \prod_{i=1}^4 \frac{\beta_i}{(j_i - \alpha_i)} A_{\alpha_1, \alpha_2, \alpha_3, \alpha_4} \quad (3.13)$$

If a Sommerfeld-Watson representation is written[16] for the corresponding multiparticle amplitude the contribution of the reggeon amplitude to a multi-Regge limit can be obtained. This limit will involve taking corresponding invariants large, say $s_i \rightarrow \infty$ $i=1, \dots, 4$. Schematically we can write



$$\equiv \prod_{i=1}^4 s_i^{\alpha_i} A_{\alpha_1, \alpha_2, \alpha_3, \alpha_4} \quad (3.14)$$

Historically a reggeon amplitude was generally defined directly this way.

Consider specifically now the reggeon associated with s_1 . We can always choose a Lorentz frame in which the limit $s_1 \rightarrow \infty$ is defined by $p_+ \rightarrow \infty, k \rightarrow k_\perp$ where p and k are the momenta labelled in Fig. 3.5 and k_\perp is the transverse momentum carried by the reggeon.

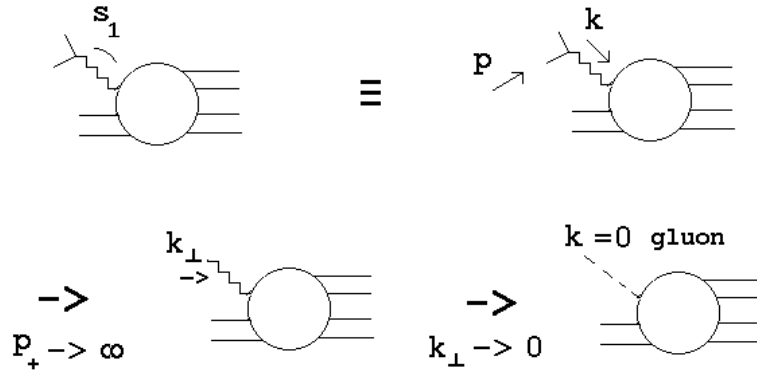


Fig. 3.5 Reduction of a Reggeon Amplitude to a Gluon Amplitude.

Since the four-momentum k is reduced to a transverse momentum k_\perp by the Regge limit, the further limit $k_\perp \rightarrow 0$ is equivalent to setting $k = 0$. Because of the reggeization of the gluon, the reggeon amplitude must give the $k = 0$ gluon amplitude. That is, as the transverse momentum of a reggeon vanishes it can be identified with an elementary gluon carrying *zero four-momentum*. The remainder of the reggeon amplitude under discussion is embedded in an on-shell S-Matrix amplitude as in (3.14) and Fig. 3.5. Therefore we obtain the zero momentum limit of the amplitude for an off-shell gluon to couple to an S-Matrix element. This amplitude satisfies a Ward identity[23].

The Ward Identity has the form

$$k_\mu \langle A_\mu(k) \dots \rangle = 0 \quad (3.15)$$

where $\langle A_\mu(k) \dots \rangle$ is the amplitude involving a gluon with momentum k_μ . To argue that $\langle A_\mu \dots \rangle$ vanishes at $k = 0$ we simply differentiate i.e.

$$\begin{aligned} \langle A_\mu \dots \rangle + \frac{\partial \langle A_\nu \dots \rangle}{\partial k_\mu} k_\nu &= 0 \\ \Rightarrow \langle A_\mu \dots \rangle \underset{(k_\mu \rightarrow 0)}{\rightarrow} 0 \quad \text{if} \quad \frac{\partial \langle A_\nu \dots \rangle}{\partial k_\mu} &\not\rightarrow \infty \end{aligned} \quad (3.16)$$

If there are no internal infra-red divergences occurring explicitly at zero transverse momentum (as will be the case in the absence of massless fermions[1]), then, as illustrated, this identity requires the amplitude to vanish. Clearly this argument can be applied to each of the reggeons in (3.14).

3.3 Color Factors

For our purposes we are interested only in SU(N) gauge theory and so we can evaluate color factors from the very simple diagrammatic identities given by C. Y. Lo[24]. These are summarized completely in Fig. 3.6.

$$\begin{array}{c}
\text{Diagram: } \begin{array}{c} i \\ | \\ j \end{array} \text{---} \begin{array}{c} | \\ k \end{array} = (2/N)^{1/2} i C_{ijk} \\
\text{Diagram: } \begin{array}{c} i \\ | \\ j \end{array} = \delta_{ij}
\end{array}$$

$$\begin{array}{c}
\text{Diagram: } \begin{array}{c} | \\ | \end{array} - \begin{array}{c} \diagup \diagdown \end{array} = \begin{array}{c} | \\ | \end{array} \\
\text{(a)}
\end{array}$$

$$\begin{array}{c}
\text{Diagram: } \begin{array}{c} | \\ | \end{array} = 2 \begin{array}{c} | \end{array} \\
\text{(b)}
\end{array}$$

$$\begin{array}{c}
\text{Diagram: } \begin{array}{c} | \\ | \end{array} = \begin{array}{c} | \end{array} \\
\text{(c)}
\end{array}$$

$$\begin{array}{c}
\text{Diagram: } \begin{array}{c} | \\ | \end{array} - \begin{array}{c} | \\ \circ \end{array} = \begin{array}{c} | \\ \circ \end{array} \\
\Rightarrow \quad 2 \begin{array}{c} | \\ | \end{array} = \begin{array}{c} | \\ \circ \end{array}
\end{array}$$

$$\text{(d)}$$

Fig. 3.6 Structure Constant Identities - (a) Jacobi Identity (b) Normalization Relation (c) Triangle Contraction (d) Triangle Contraction Derivation.

4. NONSENSE REGGEON STATES IN MULTIPARTICLE t -CHANNEL UNITARITY

In this Section we will try to give a simple, essentially self-contained, introduction to the elements of Regge theory that are needed in our analysis. We fear that for those readers with some knowledge of the formalism our approach will be too elementary, while for those with no knowledge our description will be far too short on details. Nevertheless we will try to find the best middle course we can. We will review established results on Regge cut discontinuities and also discuss reggeization via unitarity.

As we have noted, the analogue of the leading-log expansion in momentum space is an expansion around $j = 1$ in the angular momentum plane. Our aim is to show how a transverse momentum integral formalism emerges naturally from analysis of the multiparticle contributions to t -channel unitarity near this point. It will be crucial that, in a vector theory, $j = 1$ is a “nonsense” point. Consequently we begin by introducing the concept of “nonsense” states that occur, by analytic continuation,

as “intermediate states” in partial-wave amplitudes. Such states have unphysical (i.e. nonsense) angular momentum relative to the helicities of the external states to which they couple. To illustrate this and to introduce the variety of Regge theory concepts and language we use, we briefly review the formalism for the simplest possible case, that of elastic scattering.

4.1 Wrong-Signature Nonsense Poles, Right-Signature Nonsense Zeroes and Threshold Behavior

Consider the partial-wave expansion of an elastic scattering amplitude for spinless particles i.e.

$$A(z, t) = \sum_{j=0}^{\infty} (2j+1) a_j(t) P_j(z), \quad (4.1)$$

$z = \cos\theta$, where θ is the t -channel center of mass scattering angle, and the $P_j(z)$ are Legendre polynomials. The inversion formula for $a_j(t)$ is

$$\begin{aligned} a_j(t) &= \frac{1}{2} \int_{-1}^{+1} dz A(z, t) P_j(z) \\ &= \int_C dz A(z, t) Q_j(z), \end{aligned} \quad (4.2)$$

C is a contour enclosing the interval $-1 < z < 1$ and so applying Cauchy’s theorem (for j sufficiently large) gives

$$a_j(t) = \frac{1}{2\pi} \int_{I_R + I_L} dz' Q_j(z') \Delta(z', t) \quad (4.3)$$

where I_R and I_L are, respectively, the right and left-hand cuts of $A(z, t)$ and $\Delta(z, t)$ is the corresponding discontinuity. The (unique) continuation to complex j is given by using

$$Q_j(z) = (-1)^{j+1} Q_j(-z), \quad j = 0, 1, 2, \dots \quad (4.4)$$

to define “signatured” continuations from even and odd j respectively, that is

$$a_j^{\pm}(t) = [a_j^R(t) \mp a_j^L(t)] / 2, \quad (4.5)$$

where

$$a_j^R(t) = \frac{1}{2\pi} \int_{I_R} dz' Q_j(z') \Delta(z', t) \quad a_j^L(t) = \frac{1}{2\pi} \int_{I_L} dz' Q_j(-z') \Delta(z', t). \quad (4.6)$$

The asymptotic behavior of $A(z,t)$ can be studied via the Sommerfeld-Watson transformation of (4.1) i.e.

$$A(z,t) = \sum_{\pm} \int dj \frac{(2j+1)}{4\sin\pi j} a_j^{\pm}(t) \left(P_j(z) \pm P_j(-z) \right). \quad (4.7)$$

where the contour of integration is parallel with the imaginary axis. Pulling the contour to the left and picking up the singularities of $a_j(t)$ leads to an asymptotic expansion for $z \rightarrow \infty$.

Using

$$Q_j(z) \xrightarrow{j \rightarrow -1} \Gamma(j+1) \sim \frac{1}{j+1} \quad (4.8)$$

we have (formally)

$$a_j^{\pm}(t) \xrightarrow{j \rightarrow -1} \frac{1}{2\pi(j+1)} \left(\int_{I^R} \mp \int_{I^L} \right) dz' \Delta(z',t). \quad (4.9)$$

Since the external particles have helicity (and spin) zero, $j = -1$ is the first “nonsense” point i.e.

$$j = n_1 + n_2 - 1$$

where in this case $n_1 = n_2 = 0$. (4.9) shows that there is a “nonsense” pole which potentially may give a contribution to the asymptotic behavior.

We now make a crucial observation. If the amplitude is Regge-behaved, that is the asymptotic behavior is t -dependent, then the integrals over I^R and I^L can be defined for all t values by analytic continuation from a t -range where they converge[16]. In this case

$$\left(\int_{I^R} + \int_{I^L} \right) dz' \Delta(z',t) = 0 \quad (4.10)$$

- as if the amplitude satisfied an unsubtracted dispersion relation. As a result the residue of the “nonsense pole” given by (4.9) vanishes in the odd (i.e. negative) signature amplitude and so does not contribute to the asymptotic behavior. In the even-signature case the “signature factor” $1 + (-1)^j$, arising from $\left(P_j(z) \pm P_j(-z) \right)$, cancels the contribution of the pole in the asymptotic expansion obtained from (4.7). Noting that $j = -1$ is an odd integer point, we say the nonsense pole occurs only in the “wrong-signature” amplitude (i.e. the even signature amplitude).

The “threshold behaviour” of partial-wave amplitudes will also play an important role in our discussion. We can illustrate this as follows. Suppose, for the moment, that the initial and final particles have distinct masses m_i , $i = 1, \dots, 4$. In this case we have

$$\begin{aligned} s = m_1^2 + m_3^2 - & \frac{(t + m_3^2 - m_4^2)(t + m_1^2 - m_2^2)}{2t} \\ & + \frac{\lambda^{1/2}(t, m_1^2, m_2^2) \lambda^{1/2}(t, m_3^2, m_4^2)}{2t} z \end{aligned} \quad (4.11)$$

where, as usual, $\lambda(a, b, c) = a^2 + b^2 + c^2 - 2ab - 2bc - 2ac$. Close to the threshold $\lambda(t, m_1^2, m_2^2) = 0$ (or the threshold $\lambda(t, m_3^2, m_4^2) = 0$) finite s (or u) corresponds to large z . Since

$$Q_j(z) \xrightarrow[z \rightarrow \infty]{} z^{-j-1} \quad (4.12)$$

(4.3) then gives

$$a_j(t) \underset{\lambda(t, m_1^2, m_2^2) \rightarrow 0}{\sim} \left(\frac{\lambda(t, m_1^2, m_2^2)}{t} \right)^{j/2} \int ds' s'^{-j-1} \Delta(s', t) \quad (4.13)$$

If the external helicities, in the t -channel center of mass, are $(n_1, -n_2)$ for the initial state and $(n_3, -n_4)$ for the final state then, writing $n = n_1 + n_2$ and $n' = n_3 + n_4$, the generalization of (4.3) is

$$a_{jnn'}(t) = \frac{1}{2\pi} \int_{I_R+I_L} dz' (1+z')^{\frac{n+n'}{2}} (1-z')^{\frac{n-n'}{2}} e_{nn'}^j(z') \Delta(z', t) \quad (4.14)$$

$e_{nn'}^j(z)$ is a second-type $SO(3)$ representation function satisfying

$$\begin{aligned} (1+z')^{\frac{n+n'}{2}} (1-z')^{\frac{n-n'}{2}} e_{nn'}^j & \xrightarrow[j \rightarrow n-1]{} \frac{[\Gamma(j+n+1)\Gamma(j-n+1)\Gamma(j+n'+1)\Gamma(j-n'+1)]^{1/2}}{2^{1-n}\Gamma(2j+2)} \end{aligned} \quad (4.15)$$

There is now a “nonsense branch-point” at $j = n-1$ rather than the simple “nonsense pole” at $j = -1$. Since there are similar branch-points in the $d_{nn'}^j(z)$ that replace $P^j(z)$ in (4.7) the above discussion of nonsense behavior for spinless amplitudes goes

through analogously, except that (for $n \geq n'$) $j \rightarrow n - 1$ replaces $j \rightarrow -1$. The corresponding generalization of (4.13) is

$$a_{jnn'}(t) \underset{\lambda(t, m_1^2, m_3^2) \rightarrow 0}{\sim} \left(\frac{\lambda(t, m_1^2, m_3^2)}{t} \right)^{(j-n)/2} \int ds' s'^{-j+n-1} \Delta(s', t) \quad (4.16)$$

For the reggeon amplitudes with non-integer helicities ($n_1 = \alpha_1, n_2 = \alpha_2$) that appear in the following, the first nonsense point is $j = \alpha_1 + \alpha_2 - 1$. Both (4.15) and (4.16) generalize straightforwardly to the case of non-integer helicities. More details can be found in [16]. We move on now to t -channel unitarity.

4.2 Nonsense Reggeon States and Regge Cuts

We begin with the application of multiparticle t -channel unitarity to derive Regge cut discontinuities[16]. We shall see that nonsense reggeon states are a key ingredient. Although, as we described in the Introduction, the history of this formalism goes back thirty years, it is still not widely known. As an introduction we briefly review the simplest case, i.e. the derivation of the discontinuity formula for the two-reggeon cut generated by the exchange of two Regge poles. As we shall see this will give us directly the general form of the discontinuity formula (3.8) implied by the BFKL equation.

Consider the the partial-wave projection of the four-particle intermediate state contribution to the unitarity equation. We use multiparticle partial-wave amplitudes corresponding to the particular “coupling scheme” illustrated in Fig. 4.1.

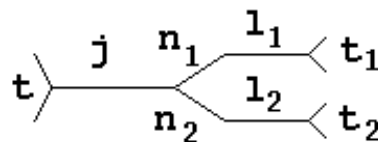


Fig. 4.1 Partial-wave coupling scheme for the 2-4 production amplitude

l_1 (l_2) and n_1 ($-n_2$) are respectively the angular momentum and helicity (in the overall center of mass) of the two-particle state with energy t_1 (t_2). (Note that we are using the same convention as in the previous sub-section. If n_1 is a positive helicity in the center of mass frame, then, n_2 is the negative of the corresponding helicity. With this convention both $j = n_1 + n_2 - 1$ and $j = -n_1 - n_2 - 1$ are nonsense values of j .)

The partial-wave projection of the four-particle unitarity contribution is

$$a_j(t) - a_j^i(t) = \int d\rho \sum_{|n_1+n_2| \leq j} \sum_{l_1 \geq |n_1|} \sum_{l_2 \geq |n_2|} a_{j\tilde{l}n}(t, \tilde{t}) a_{j\tilde{l}n}^i(t, \tilde{t}) \quad (4.17)$$

where i denotes an amplitude evaluated on the unphysical side of the four-particle branch-cut. (We will avoid discussing subtleties associated with the definition of i amplitudes, in particular the specification of the additional boundary-values involved.) If all particles have mass m , but are not identical,

$$\begin{aligned} \int d\rho(t, t_1, t_2) &= \frac{i}{(2\pi)^5 2^6} \int dt_1 dt_2 \\ &\times \left[\frac{\lambda^{1/2}(t, t_1, t_2)}{t} \right] \left[\frac{\lambda^{1/2}(t_1, m^2, m^2)}{t_1} \right] \left[\frac{\lambda^{1/2}(t_2, m^2, m^2)}{t_2} \right] \end{aligned} \quad (4.18)$$

with the integration region defined by $\lambda \geq 0$, for each of the three λ functions.

The basis for all of the following analysis is the continuation of unitarity partial-wave projections such as (4.17) to complex j . It was clear from the original *GPT* paper[14] that this would provide a very powerful general analysis tool - provided the correct unique form for the continuation is found. The essential tool we use is (signatured versions of) the identity

$$\begin{aligned} \sum_{\substack{n_1 \geq 0, n_2 \geq 0 \\ j \geq n_1 + n_2}} F(j, n_1, n_2) &= - \frac{\sin \pi j}{2^2} \int_{C_j} \frac{dn_1 dn_2}{\sin \pi n_1 \sin \pi n_2 \sin \pi(j - n_1 - n_2)} F(j, n_1, n_2) \\ &\equiv - \Gamma_{[j]}[F(j, n_1, n_2)] \end{aligned} \quad (4.19)$$

which holds when j is an integer, if the integration contour is defined as a function of j such that, for $j \sim -1/2$, $C_j \equiv [n_r = -1/4 + i\nu_r, -\infty < \nu_r < \infty, r = 1, 2]$, and is defined for general values of j by analytic continuation. Note that (4.19) sums explicitly only the positive values of both n_1 and n_2 . For the full unitarity equation, each combination of signs has to be treated separately and gives a distinct contribution to the continuation in j . Nonsense states with $n_1, n_2 > 0$ and $j = n_1 + n_2 - 1$ will appear in the contribution we discuss explicitly. Nonsense states with $n_1, n_2 < 0$, will appear in a separate contribution. In much of our discussion we will not refer explicitly to this and we will implicitly sum over helicity signs.

We will discuss only contributions from odd signature reggeons (gluons) and so consider only odd-signature values of n_1 and n_2 . In this case we replace $\sin \pi n_{1,2}$

by $2 \sin\frac{\pi}{2}(n_{1,2} - 1)$ in (4.19). We will consider both even and odd signature in j and so define

$$\begin{aligned} \Gamma_{[j]}^{\pm} &= \frac{1}{2^4} \sin\frac{\pi}{2}(j - \sigma^{\pm}) \int dn_1 dn_2 \\ &\quad \times \frac{1}{\sin\frac{\pi}{2}(j - \sigma^{\pm} - n_1 - n_2 + 2) \sin\frac{\pi}{2}(n_1 - 1) \sin\frac{\pi}{2}(n_2 - 1)} \end{aligned} \quad (4.20)$$

where $\sigma^+ = 0$ and $\sigma^- = 1$. $\Gamma_{(j)}^{\pm}$ reduces to a finite sum when j is an even/odd integer respectively.

To discuss the generation of Regge cuts, we suppose there are Regge poles at $l_{1,2} = n_{1,2} = \alpha(t_{1,2}) \equiv \alpha_{1,2}$ in the production amplitude partial waves. This is represented diagrammatically in Fig. 4.2

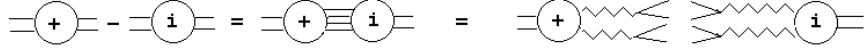


Fig. 4.2 Regge poles in the production amplitude.

(We should, perhaps, comment that if a Regge pole is present in elastic amplitudes, its' presence in production amplitudes can actually be proved[16].) After utilising two-particle unitarity in both the t_1 and t_2 subchannels, we can write the relevant part of the j -plane continuation of (4.17) as

$$a_j^{\pm} - a_j^{\pm i} = - \Gamma_{(j)}^{\pm} \left[\int d\tilde{\rho}(t, t_1, t_2) A_{\alpha}^{\pm}(j, t) A_{\alpha}^{\pm i}(j, t) \Big/ (n_1 - \alpha_1)(n_2 - \alpha_2) \right] \quad (4.21)$$

where $A_{\alpha}^{\pm}(j, t) \equiv A_{\alpha_1, \alpha_2}^{\pm}(j, t)$ is the production amplitude Regge pole residue and

$$\int_{C_1, C_2} d\tilde{\rho}(t, t_1, t_2) = \frac{i}{2^5 \pi^3} \int_{C_1, C_2} dt_1 dt_2 \left[\frac{\lambda^{1/2}(t, t_1, t_2)}{t} \right] \quad (4.22)$$

As a consequence of the two-particle unitarity manipulations, C_1 and C_2 are contour integrals beginning and ending at $\lambda = 0$ and circling, respectively, the thresholds at $t_1 = 4m^2$ and $t_2 = 4m^2$. For our purposes it will be important only that $\lambda = 0$ is a boundary of the integration region. It is important (from a more general point of view) that the integral is over a finite range of t_1 and t_2 i.e. it does not extend to infinite values of the transverse momentum variables that we introduce below.

We now use the Regge poles at $n_1 = \alpha_1$ and $n_2 = \alpha_2$ to perform the n_1 and n_2 integrations. As we discussed above, there is a “nonsense branch-point” factor $(j - \alpha_1 - \alpha_2 + 1)^{-1/2}$ in $A_{\tilde{\alpha}}^\pm$. For the present discussion, we extract this factor from both $A_{\tilde{\alpha}}^\pm$ and $A_{\tilde{\alpha}}^{\pm i}$ and define (“nonsense”) residue amplitudes $G_{\tilde{\alpha}}^\pm$ and $G_{\tilde{\alpha}}^{\pm i}$. We can then rewrite (4.21) as

$$a_j^\pm - a_j^{\pm i} = \Gamma_{(j,t)}^\pm \left[G_{\tilde{\alpha}}^\pm G_{\tilde{\alpha}}^{\pm i} \right] + \dots \quad (4.23)$$

where now

$$\begin{aligned} \Gamma_{(j,t)}^\pm &= \frac{\pi^2}{4} \sin \frac{\pi}{2} (j - \sigma^\pm) \int \frac{d\tilde{\rho}}{(j - \alpha_1 - \alpha_2 + 1)} \\ &\times \frac{1}{\sin \frac{\pi}{2} (j - \alpha_1 - \alpha_2 + 2 - \sigma^\pm) \sin \frac{\pi}{2} (\alpha_1 - 1) \sin \frac{\pi}{2} (\alpha_2 - 1)} \end{aligned} \quad (4.24)$$

We observe that a branch point is potentially generated in $\Gamma_{(j,t)}^\pm$ when the pole at $j = \alpha_1 + \alpha_2 - 1$ is tangent to the phase space boundary at $\lambda = 0$. This happens when $t_1 = t_2 = t/4$ and the result is the “two-reggeon” branch-point at

$$j = 2\alpha\left(\frac{t}{4}\right) - 1 . \quad (4.25)$$

(It is important that a branch-point is also generated at $j = 2\alpha^*\left(\frac{t}{4}\right) - 1$ by that part of the contour below the particle thresholds but is present in i -amplitudes only.)

If the branch-point is indeed to be generated, there must be no “nonsense zero” in $G_{\tilde{\alpha}}$. It follows from the signatured form of (4.14) that there is no zero if the signature of $G_{\tilde{\alpha}}$, and therefore the signature of the Regge cut, is the product of the signatures of the participating Regge poles. In particular, if the Regge pole signatures are identical, the Regge cut has even signature. (Note that other j -dependent “reggeon-particle” singularities are also generated in (4.24) but only the two-reggeon cut survives[25, 26, 2] on the physical sheet for $t \sim 0$).

If neither $G_{\tilde{\alpha}}^+$ or $G_{\tilde{\alpha}}^{+i}$ contained the Regge cut, the discontinuity would simply be given by

$$\delta_j a^+(j) = \delta_j \left\{ \Gamma_{(j,t)}^+ \right\} \left[G_{\tilde{\alpha}}^+ G_{\tilde{\alpha}}^{+i} \right], \quad (4.26)$$

where δ_j denotes the discontinuity across the cut and $\delta_j \{ \Gamma^+(j, t) \}$ is obtained from $\Gamma_{(j,t)}^+$ by writing

$$(j - \alpha_1 - \alpha_2 + 1)^{-1} \rightarrow 2\pi i \delta(j - \alpha_1 - \alpha_2 + 1) . \quad (4.27)$$

i.e.

$$\begin{aligned} \delta_j \{ \Gamma^+(j, t) \} &= \frac{\pi^3}{2} \sin \frac{\pi}{2} j \int d\tilde{\rho} \delta(j - \alpha_1 - \alpha_2 + 1) \\ &\times \frac{1}{\sin \frac{\pi}{2} (j - \alpha_1 - \alpha_2 + 2) \sin \frac{\pi}{2} (\alpha_1 - 1) \sin \frac{\pi}{2} (\alpha_2 - 1)} \end{aligned} \quad (4.28)$$

In fact $G_{\tilde{\alpha}}^+(j, t)$ does contain the cut, but it is absent in all i -amplitudes. (As we have already remarked, these amplitudes have a branch-point at the complex conjugate location). Consequently, after a nontrivial extension of the analysis to amplitudes with reggeons as external states[16], a standard unitarity manipulation gives the full discontinuity in the form

$$\delta_j a^+(j) = \delta_j \{ \Gamma_{(j,t)}^+ \} \left[G_{\tilde{\alpha}}^+(j^+, t) G_{\tilde{\alpha}}^+(j^-, t) \right], \quad (4.29)$$

where j^\pm denotes that the amplitude is evaluated above or below the reggeon cut involved. The discontinuity formula (4.29) holds for general external states, including the case when they are all reggeons.

To define an amplitude with all external reggeons, i.e. a full reggeon scattering amplitude, we proceed as anticipated in the last Section. We first partial-wave project a four-four amplitude according to the coupling scheme shown in Fig. 4.3.

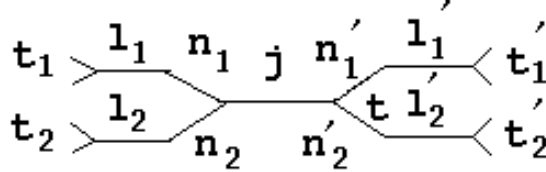


Fig. 4.3 Coupling scheme for the 4-4 amplitude

After continuation to complex angular momenta and helicities we then extract the multi-Regge pole residue at $l_1 = n_1 = \alpha_1$, $l_2 = n_2 = \alpha_2$, $l'_1 = n'_1 = \alpha'_1$, $l'_2 = n'_2 = \alpha'_2$.

After factorising off the couplings of the Regge poles to the external particles we obtain a reggeon scattering amplitude.

We can write a self-contained “reggeon unitarity” equation as follows. We first define “nonsense” reggeon scattering amplitudes by extracting all the nonsense and threshold factors appearing in (4.15) and (4.16). That is we write

$$\begin{aligned} \mathcal{G}_{\tilde{\alpha}\tilde{\alpha}'}^{\pm}(j, t) &= [(j - \alpha_1 - \alpha_2 + 1)(j - \alpha'_1 - \alpha'_2 + 1)]^{1/2} \\ &\times \left[\frac{\lambda(t, t_1, t_2)}{t} \right]^{-(j - \alpha_1 - \alpha_2)/2} \left[\frac{\lambda(t, t'_1, t'_2)}{t} \right]^{-(j - \alpha'_1 - \alpha'_2)/2} A_{\tilde{\alpha}\tilde{\alpha}'}^{\pm}(j, t) \end{aligned} \quad (4.30)$$

where $A_{\tilde{\alpha}\tilde{\alpha}'}^{\pm}(j, t) \equiv A_{\alpha(t_1), \alpha(t_2), \alpha(t'_1), \alpha(t'_2)}^{\pm}(j, t)$ is a full reggeon scattering amplitude.

We then combine the threshold factors with $\Gamma_{(j,t)}^+$ to define

$$\tilde{\Gamma}_{(j,t)}^+ = \Gamma_{(j,t)}^+ \left[\frac{\lambda(t, t_1, t_2)}{t} \right]^{(j - \alpha_1 - \alpha_2)} \quad (4.31)$$

so that (4.29) gives

$$\mathcal{G}_{\tilde{\alpha}\tilde{\alpha}'}^+(j^+, t) - \mathcal{G}_{\tilde{\alpha}\tilde{\alpha}'}^-(j^-, t) = \delta_j \left\{ \tilde{\Gamma}_{(j,t)}^+ \right\} \left[\mathcal{G}_{\tilde{\alpha}\tilde{\alpha}'}^+(j^+, t) \mathcal{G}_{\tilde{\alpha}\tilde{\alpha}'}^-(j^-, t) \right], \quad (4.32)$$

where now

$$\begin{aligned} \delta_j \left\{ \tilde{\Gamma}_{(j,t)}^+ \right\} &= \frac{\pi}{2} \sin \frac{\pi}{2} j \int d\tilde{\rho} \left[\frac{\lambda(t, t_1, t_2)}{t} \right]^{-1} \delta(j - \alpha_1 - \alpha_2 + 1) \\ &\times \frac{1}{\sin \frac{\pi}{2} (j - \alpha_1 - \alpha_2 + 2) \sin \frac{\pi}{2} (\alpha_1 - 1) \sin \frac{\pi}{2} (\alpha_2 - 1)} \end{aligned} \quad (4.33)$$

which already compares closely with the discontinuity formula (3.8) given by the BFKL equation.

We can simplify $\tilde{\Gamma}_{(j,t)}^+$ considerably if we analytically continue to $t \sim 0$. The relevant part of the phase-space is then $t_1 \sim t_2 \sim 0$. If we make a linear approximation to the trajectory function, i.e. $\alpha_r = 1 + \alpha' t_r + \dots$, then we can take $\sin \frac{\pi}{2} (\alpha_r - 1) \sim \pi \alpha' t_r / 2$ and since $j \sim 1$ we have $\sin \frac{\pi}{2} j \sim 1$. If we also absorb a factor of $(\alpha')^{-1}$ in the definition of $\mathcal{G}_{\tilde{\alpha}\tilde{\alpha}'}$ we obtain by combining (4.22) with (4.33)

$$\delta_j \left\{ \tilde{\Gamma}_{(j,t)}^+ \right\} = \frac{1}{2^4 \pi^2} \int \frac{dt_1 dt_2}{\lambda^{1/2}(t, t_1, t_2)} \frac{1}{t_1 t_2} \delta(j - \alpha_1 - \alpha_2 + 1) \quad (4.34)$$

Finally we change to two-dimensional ‘‘transverse momentum’’ variables defined, for our present purposes, by

$$t = q^2, \quad t_1 = k^2, \quad t_2 = (q - k)^2 \quad (4.35)$$

(As we remarked already in the Introduction, the time-like two-dimensional integrals that we utilise, analytically continue[27] into the corresponding integrals over the usual transverse momentum variables in the negative t region.)

The jacobian for the transformation (4.35) is

$$\frac{dt_1 dt_2}{\lambda^{1/2}(t, t_1, t_2)} = 2d^2 k \quad (4.36)$$

If we also write $\omega = j - 1$ and $\Delta_r = 1 - \alpha_r$ we can write

$$\delta_j \left\{ \tilde{\Gamma}_{(j,t)}^+ \right\} \equiv \delta_\omega \left\{ \tilde{\Gamma}_{(\omega,q^2)}^+ \right\} \quad (4.37)$$

where now

$$\tilde{\Gamma}_{(\omega,q^2)}^+ = \frac{1}{2^4 \pi^3} \int \frac{d^2 k}{k^2 (k - q)^2} \frac{1}{\omega - \Delta_1 - \Delta_2} \quad (4.38)$$

which we anticipated in (2.3), i.e. the discontinuity formula for the two-reggeon cut is expressed as a transverse momentum integral of the form that is obtained directly from high-energy calculations. Indeed once (4.37) and (4.38) are utilised, (3.8) compares directly with (4.32), apart from a factor of i from $\Gamma_{(j,t)}^+$ due to the analytic continuation in t . Note that the threshold factors in (4.31), evaluated at the nonsense point, are crucial in producing the correct jacobian. This explains, from the view-point of t -channel unitarity, why direct Regge-limit calculations produce transverse-momentum integrals. Such integrals are naturally produced by the exchange of t -channel nonsense states.

As we emphasized in Section 3, the discontinuity formula is satisfied independently of the form of the kernel. Given that the gluon reggeizes in leading log, it is then a consequence of t -channel unitarity that *an evolution equation, having the general form of the BFKL equation, is satisfied by the next-to-leading log results*. Our goal is, of course, to also derive the particular form of the kernel from general unitarity arguments combined with Ward identity constraints. To do this we will have to add the extra ingredients of expanding around $j = 1$ and extracting particle threshold singularities in t . Neither of which is necessary to obtain Regge cut discontinuity formulae.

The above analysis of the two-reggeon cut generalises straightforwardly to the analysis of the N -reggeon cut - which originates from a nonsense state of N -reggeons i.e. $j = \sum_{r=1}^N \alpha_r - N + 1$. A self-contained set of reggeon unitarity equations can be written for multireggeon scattering amplitudes of both signatures with the signature of the Regge cut due to N reggeized gluons being $(-1)^N$. All the multireggeon discontinuity formulae can be written in terms of transverse momentum integrals. We emphasize that this is a property of the phase-space generating the branch-point and is not a perturbative result. In writing (4.38) we implicitly extended the transverse momentum integrations to infinity. For the discontinuity formula the upper end point is irrelevant, as it is, analogously, for all multi-reggeon discontinuity formulae. Since the transverse momentum integrals that arise in high-energy calculations always extend to infinity we write our integrals in the same way. Nevertheless it is important to emphasize that t -channel unitarity gives finite integrals. In particular, when gluons are massless all the structure is at $t = 0$

4.3 The Trajectory Function as a Nonsense Threshold

As we now begin to discuss, there are also well-defined reggeon contributions with signature $(-1)^{N-1}$, i.e. the opposite signature to the Regge cut they generate. Such contributions give thresholds in t rather than in j . Indeed it will be crucial for the emergence of higher-order kernels from our analysis that reggeons can simultaneously participate in the generation of Regge cuts and in the generation of thresholds in t . We shall find that in the simplest cases, it is clear that only nonsense-point kinematics is involved and this leads directly to transverse momentum integrals for the threshold contributions. However, as we go to higher-orders this will be a subtle issue that we will need to discuss carefully. We will set up our general discussion by first describing how the leading-log reggeization of the gluon can be seen as a threshold contribution of the two-reggeon state.

From (4.24) we see that there is an additional pole at the nonsense point in the odd-signature phase-space (from the factor of $\sin\frac{\pi}{2}(j - \alpha_1 - \alpha_2 + 1)$ in the denominator) giving

$$\Gamma_{(j,t)}^- = \frac{\pi}{2} \sin\frac{\pi}{2}(j - 1) \int \frac{d\tilde{\rho}}{[j - \alpha_1 - \alpha_2 + 1]^2 [\sin\frac{\pi}{2}(\alpha_1 - 1)][\sin\frac{\pi}{2}(\alpha_2 - 1)]} \quad (4.39)$$

In writing (4.39) we have extracted nonsense branch-point factors as in the last subsection. From (4.15) and a generalization of the dispersion relation argument following (4.10), there must be linear nonsense zeroes in both $G_{\alpha}^-(j, t)$ and $G_{\alpha}^{-i}(j, t)$. These

cancel the double pole in (4.39) and so no Regge cut is generated. Instead we now focus on the threshold singularity in t which is generated in $\Gamma_{(j,t)}^-$ when

$$\begin{aligned}\alpha_1 &\equiv \alpha(t_1) = 1, \quad \alpha_2 \equiv \alpha(t_2) = 1, \\ \lambda(t, t_1, t_2) &= 0.\end{aligned}\tag{4.40}$$

This threshold is similarly generated in the positive signature phase-space and becomes relevant at non-leading log, although we will not discuss it in this paper.

(There is a general point underlying the following analysis which we should note at this point. Two massless gluons can not form a physical massless state with $j = 1$, whereas a nonsense state can have $j = 1$ as a result of analytic continuation. This is why the leading (i.e. most singular) behavior at a t -channel threshold will come from nonsense states coupling via the three-reggeon vertex - when they can contribute.)

Assuming that the threshold does not appear in i -amplitudes (we discuss conditions under which this will be the case below) we can derive a discontinuity formula analogous to (4.26) i.e.

$$\delta_t \left[\mathcal{G}_{\alpha''\alpha'}^-(j, t) \right] = \delta_t \left\{ \tilde{\Gamma}_{(j,t)}^- \right\} \left[\mathcal{G}_{\alpha''\alpha'}^-(j, t^+) \mathcal{G}_{\alpha\alpha'}^-(j, t^-) \right],\tag{4.41}$$

where $\mathcal{G}_{\alpha''\alpha'}^-(j, t)$ is again defined by (4.30) and we have defined $\tilde{\Gamma}_{(j,t)}^-$ in analogy with the definition of $\tilde{\Gamma}_{(j,t)}^+$ in (4.31). We obtain a simple expression for $\tilde{\Gamma}_{(j,t)}^-$ if we set $\alpha_1 = \alpha_2 = 1$ and consider the leading dependence of (4.41) as $j \rightarrow 1$. Since $j = 1$ is now the nonsense point relevant for the phase-space integration, for the leading threshold behavior due to $\lambda(t, t_1, t_2) \rightarrow 0$ we can write, in analogy with (4.34)-(4.38),

$$\delta_t \left\{ \tilde{\Gamma}_{(j,t)}^- \right\} \equiv \frac{1}{j-1} \delta_{q^2} \left\{ \tilde{\Gamma}_{(q^2)}^- \right\} = \frac{1}{\omega} \delta_{q^2} \left\{ J_1(q^2) \right\}\tag{4.42}$$

where $J_1(q^2)$ is defined by (2.5).

Consider now the implications of (4.41) when $\alpha_r \rightarrow 1$, (i.e. $t_r \rightarrow 0$) $r = 1, \dots, 4$, so that $j \sim 1$ is also a nonsense-point for the external helicities. There are two important features of $\mathcal{G}^-(j, t)$ ($\equiv \mathcal{G}_{1111}^-(j, t)$) that we have already discussed.

Namely the presence of the reggeized gluon, implying a factor $(\omega - \Delta(q^2))^{-1}$ and the nonsense zero, implying a factor of ω . We have not yet discussed the Ward identity constraints.

This is the first point at which it becomes important to impose gauge invariance on the form of our amplitudes. Because of the Ward identity constraints discussed in Section 3, the reggeon amplitudes we are discussing must vanish when any $k_r \rightarrow 0$, $r = 1, \dots, 4$. The k_r are two dimensional momenta with $t_r = k_r^2$. Since we have already set $k_1^2 = k_2^2 = k_3^2 = k_4^2 = 0$, it follows that

$$q^2 = (k_1 + k_2)^2 = 2k_1 \cdot k_2 = (k_3 + k_4)^2 = 2k_3 \cdot k_4 \quad (4.43)$$

and so a factor of q^2 will satisfy the constraint. Since \mathcal{G}^- has the (transverse momentum) dimensions of q^2 , we suppose that

$$\mathcal{G}^-(j, t) \equiv \mathcal{G}^-(\omega, q^2) = \frac{g^2 \omega q^2}{(\omega - \Delta(q^2))} \quad (4.44)$$

where g can be treated as a constant. g is defined, at this point, as a “triple Regge” coupling of a single reggeized gluon to two gluons in a nonsense state.

To introduce the “gauge group” into our discussion we suppose there is a global “color symmetry” of the reggeon spectrum. In particular we assume that the reggeized “gluon” belongs to the adjoint representation of $SU(N)$. That is there are $N^2 - 1$ reggeons with coupling c_{ijk} g , $i, j, k, = 1, 2, \dots, N^2 - 1$. The triple Regge coupling is then

$$g c_{ijk} \quad (4.45)$$

where we identify the c_{ijk} with the usual group structure constants. (4.44) becomes

$$G_{i_1, i_2, i_3, i_4}^-(j, t) \equiv G^-(\omega, q^2) = \frac{g^2 \sum_{n=1}^N c_{n i_1 i_2} c_{n i_3 i_4} \omega q^2}{(\omega - \Delta(q^2))} \quad (4.46)$$

If we reinstate the nonsense factors we have extracted in (4.30) (this will remove the explicit nonsense-zero factor of ω) and set $\alpha' = 0$, this is exactly the nonsense amplitude that is obtained [20] by direct $O(g^2)$ calculations.

It is now clear that the lowest-order nonsense reggeon scattering amplitude (4.46) is entirely determined by the following general properties i.e.

- reggeization
- the color structure of the triple Regge vertex
- the nonsense zero
- the Ward identity constraint

each of which is represented by a simple factor. If we initially take $\Delta(q^2) = \alpha' q^2$ then at the Regge pole we can formally factorize the residue i.e.

$$g^2 \omega q^2 \rightarrow g^2 \alpha'(q^2)^2 \quad (4.47)$$

and obtain the full triple reggeon vertex

$$r_{ijk}^0 = g c_{ijk} (\alpha')^{1/2} q^2 \quad (4.48)$$

that we utilised in [7]. This shows that the momentum factor can be both interpreted as a nonsense zero and as due to the Ward identity constraint. We saw in [7], and will discuss further shortly, that g can, of course, also be identified as the bare gauge coupling when comparisons are made with perturbation theory.

As we have defined it, the triple Regge coupling is necessarily antisymmetric. We have identified it as a 1-2 reggeon coupling, but the 2-reggeon state is not symmetric with respect to interchange of the two reggeons. It is a nonsense state in which one reggeon carries (center of mass) helicity +1 and the other carries helicity -1. Interchanging the two reggeons amounts to a parity transformation - flipping the helicities of all three reggeons. If the reggeized gluon is a normal vector then this transformation must produce a change of sign i.e. the coupling should be anti-symmetric. We find it interesting that the antisymmetric nonabelian gauge coupling is naturally defined as a triple-Regge coupling. It certainly endorses the concept of defining reggeon non-abelian gauge theories directly. The inter-relation of the anti-symmetry of the coupling with helicity-flip change of sign will play an important role in the next Section.

We now look for corrections to the trajectory function of $O(g^2)$. For simplicity we initially omit the group structure. If we write $\Delta(q^2) = \alpha' q^2 + g^2 \Delta^1(q^2)$ then, from (4.29), we obtain

$$\frac{1}{\omega - \Delta(q^2)} - \frac{1}{\omega - \Delta^*(q^2)} = \frac{g^2 q^2 \delta_{q^2} \{ \Gamma_{q^2}^- \}}{(\omega - \Delta(q^2))(\omega - \Delta^*(q^2))} \quad (4.49)$$

giving directly

$$\delta_{q^2} \left\{ \Delta^1(q^2) \right\} = q^2 \delta_{q^2} \left\{ \Gamma^-(q^2) \right\} \quad (4.50)$$

Clearly the limit $\alpha' \rightarrow 0$ is now harmless and the solution of (4.50) is the “perturbative” reggeon trajectory. In this simple case the most obvious solution of the discontinuity formula immediately gives the full leading-log momentum-space result.

$$\alpha(q^2) = 1 + \frac{g^2}{16\pi^3} q^2 J_1(q^2) \quad (4.51)$$

Including the group structure gives

$$\begin{aligned} \alpha(q^2) &= 1 + g^2 \sum_{j,k} c_{i,j,k}^2 q^2 J_1(q^2) \\ &= 1 + g^2 N q^2 J_1(q^2) \end{aligned} \quad (4.52)$$

where we have used the diagrammatic relation of Fig. 3.5(b). From this last form of the trajectory function it is immediately clear that g can be directly identified with the bare gauge coupling.

To prepare for our analysis in the following Sections we note that we could also have deduced (4.50) from a discontinuity formula of the form

$$\delta_t [a(j, t)] = \delta_t \left\{ \tilde{\Gamma}_{(j,t)}^- \right\} \left[G_{\tilde{\alpha}}(j, t^+) G_{\tilde{\alpha}}(j, t^-) \right], \quad (4.53)$$

in which $a(j, t)$ is any scattering amplitude containing the gluon Regge pole. (4.50) follows provided only that the coupling of the gluon pole to the reggeons producing the discontinuity is given by (4.48). The pole residues in $a(j, t)$ simply factorize off and are irrelevant,

The original t -channel unitarity demonstration[20] used the two-particle equation continued to nonsense points - with the particles being those on the reggeon trajectories. The analysis we have just given is equivalent (apart from the fact that we have determined the lowest-order nonsense amplitudes from general principles) but generalises straightforwardly to allow us to discuss “multiparticle nonsense states” where the particle lies on a Regge trajectory. As we shall see, it also allows us to discuss the simultaneous participation of a reggeon in the generation of a Regge cut and a t -channel threshold. Such configurations will, in higher orders, produce a general structure of threshold singularities in reggeon interactions.

The reggeon trajectory function can be regarded as the very simplest reggeon interaction, i.e. the 1-1 interaction. Having extracted the lowest-order result for this simplest interaction from unitarity we focus on those features of the analysis that generalize in the following. The first step was to extract the threshold behavior from the partial-wave amplitudes and obtain the discontinuity in t . Then, with the aid of Ward identity constraints, we expanded both about the nonsense point $j = 1$ and in powers of g^2 . (The results, of course, demonstrate that this is equivalent to the leading-log expansion in momentum space.) The threshold behavior appearing in (4.31) implied that we had to be at the nonsense point to obtain the right jacobian for transformation to transverse momentum variables. We expect that if we keep higher powers of $(j - 1)$ in the expansion about the nonsense point, we will obtain the equivalent of momentum space non-leading log amplitudes. Higher nonsense states will couple with higher powers of g^2 and naturally produce non-leading log interactions. However, from (4.31) we see that this expansion will also contain factors of $\log[\lambda^{1/2}(t_i, t_j, t_k)]$, where the $t_{i,j,k}$ are (the square of) momenta carried by reggeons. *To represent such effects in terms of transverse momentum diagrams it will be necessary to include, as a breaking of scale invariance, logarithms of the transverse momenta involved.* We will not discuss such effects in this paper.

So far the role of α' has been only to anticipate perturbative reggeization effects that “aposteori” justify the use of the reggeon formalism. To recover perturbation theory we simply set $\alpha' = 0$. Justification of our analysis of the t -thresholds actually requires that we both distinguish the particle thresholds due to reggeons from those appearing in the initial unitarity equation and have these thresholds appear at distinct locations above and below the unitarity branch points (below being denoted by “ i ” in the above). To satisfy these requirements we could assume that the unitarity states we are discussing initially are those of very light particles (perhaps “Higgs” scalars) whose presence in the theory makes the gluons both massive and unstable so that

$$\alpha(t) = 1 - \epsilon + \alpha' t + \dots \quad (4.54)$$

If we assume that ϵ has an imaginary part (due to the light particle thresholds) the sign of which is reversed below unitarity cuts, then the above discussion will go through. Our interest is in massless QCD and so at the end of our analysis we will, of course, assume that both parameters can be smoothly set to zero. (If we appeal to light particles then this assumes that they can be decoupled smoothly so that only the unitarity contributions of gluon reggeons and particles remain. Essentially the same assumption is made in s -channel unitarity calaculations.) As is already clear

from the above, in much of our discussion ϵ and α' will not play an explicit role and we will omit them. In particular, we will omit ϵ entirely.

5. THE BFKL KERNEL FROM THREE REGGEON NONSENSE STATES

In this Section we recover the $O(g^2)$ kernel described in Section 2 using the reggeon formalism of the previous Section. We consider the two-two reggeon interaction produced by the three-reggeon nonsense state. Our procedure will parallel that used to discuss the trajectory function in the last Section. We first isolate the three-particle discontinuity formula then, after constructing the lowest-order nonsense amplitudes from general arguments, use the discontinuity formula to generate the lowest-order imaginary part of the interaction.

We consider the six-particle unitarity integral and analyse it with partial-wave amplitudes corresponding to the coupling scheme shown in Fig. 5.1.

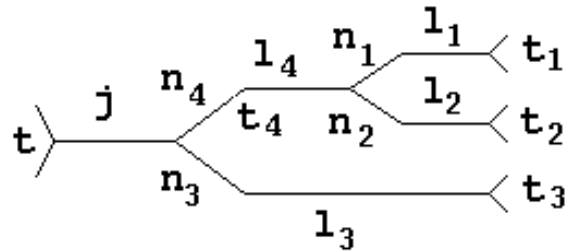


Fig. 5.1 Coupling scheme for the 2-6 production amplitude

The partial-wave projection of the unitarity integral is

$$a_j(t) - a_j^i(t) = \int d\rho \sum_{|n_3+n_4| \leq j} \sum_{|n_1+n_2| \leq l_4} \sum_{l_1 \geq |n_1|} \sum_{l_2 \geq |n_2|} \sum_{l_3 \geq |n_3|} \sum_{l_4 \geq |n_4|} \times a_{j\tilde{l}\tilde{n}}(t, \tilde{t}) a_{j\tilde{l}\tilde{n}}^i(t, \tilde{t}) \quad (5.1)$$

where i now denotes amplitudes evaluated below the six-particle cut. We consider the even signature partial-wave amplitude and keep only the terms with $l_r = n_r$, $r = 1, \dots, 4$. We will initially pick out the contribution of the nonsense pole at $j = n_3 + n_4 - 1$ and the Regge poles at $l_r = \alpha_r = \alpha(t_r)$, $r = 1, 2, 3$, that produce the three-particle threshold. The two-reggeon cut that appears in $a_j(t)$ is produced in the unitarity integral by the α_3 and α_4 Regge poles in combination with the nonsense pole.

The helicity integrals arising from the continuation to complex j of the helicity sums in (5.1) are (from even signature in j and odd signature in the n_r)

$$\begin{aligned} & \frac{1}{2^8} \sin \frac{\pi}{2} j \int \frac{dn_3 dn_4}{\sin \frac{\pi}{2} (j - n_3 - n_4) \sin \frac{\pi}{2} (n_3 - 1)} \\ & \int \frac{dn_1 dn_2}{\sin \frac{\pi}{2} (n_4 - n_1 - n_2 + 1) \sin \frac{\pi}{2} (n_1 - 1) \sin \frac{\pi}{2} (n_2 - 1)} \end{aligned} \quad (5.2)$$

If we again extract the nonsense factors implied by (4.15) (we will discuss shortly why the nonsense points dominate our analysis) we obtain

$$\begin{aligned} \Gamma_{3(j)}^+ &= \frac{1}{2^7 \pi} \int \frac{dn_3 dn_4}{(j - n_3 - n_4 + 1) \sin \frac{\pi}{2} (n_3 - 1)} \\ & \int \frac{dn_1 dn_2}{(n_4 - n_1 - n_2 + 1)^2 \sin \frac{\pi}{2} (n_1 - 1) \sin \frac{\pi}{2} (n_2 - 1)} \end{aligned} \quad (5.3)$$

Replacing j by n_4 , the structure of the n_1 and n_2 integrations is the same as for Γ^- in (4.24) - except that there is no factor of $\sin \frac{\pi}{2} (n_4 - 1)$. Correspondingly, both of the (analytically continued) partial-wave amplitudes $a_{j \tilde{l} n}$ and $a_{j \tilde{l} n}^i$ have nonsense zeros

at $l_4 = n_4 = n_1 + n_2 - 1$. These zeroes eliminate the double pole in (5.3) and ensure that no three reggeon cut is generated. As we discussed in the last Section, and will exploit below when we extract Regge pole residues, this zero can be identified with the zero of the triple reggeon vertex.

We now use the Regge poles to perform the helicity integrals over n_1 , n_2 and n_3 in (5.3). We perform the n_4 integration by picking up the nonsense-pole at $j = n_3 + n_4 - 1$. After we use two-particle unitarity to eliminate the phase-space integrations for the two particle states to which the α_1 , α_2 and α_3 Regge poles couple, the remaining phase-space integration given by the unitarity integral is a product of integrations of the form of (4.22) i.e.

$$\int d\tilde{\rho}(t, t_1, t_2, t_3, t_4) = \int_{\lambda(t, t_3, t_4) > 0} d\tilde{\rho}(t, t_3, t_4) \int_{\lambda(t_4, t_1, t_2) > 0} d\tilde{\rho}(t_4, t_1, t_2) \quad (5.4)$$

The only boundaries of the integration region that matter for us are those we have indicated, at $\lambda(t, t_3, t_4) = 0$ and $\lambda(t_4, t_1, t_2) = 0$.

Combining (5.3) and (5.4) and extracting the nonsense zeroes we can write

the three reggeon contribution to the j -plane continuation of (5.1) in the form

$$\Gamma_{3[j,t]}^+ \tilde{A}_{\tilde{\alpha}}(j,t) \tilde{A}_{\tilde{\alpha}}^i(j,t) \quad (5.5)$$

where $\tilde{A}_{\tilde{\alpha}}(j,t)$ and $\tilde{A}_{\tilde{\alpha}}^i(j,t)$ are reggeon amplitudes defined at $n_1 = \alpha_1$, $n_2 = \alpha_2$,

$n_3 = \alpha_3$ and $n_4 = j - \alpha_3 + 1$ (the notation \tilde{A}_{\dots} denotes that the nonsense zero has been extracted) and

$$\Gamma_{3[j,t]}^+ = \frac{\pi^3}{2^3} \int d\tilde{\rho} \frac{1}{\sin^{\pi/2}(\alpha_1 - 1) \sin^{\pi/2}(\alpha_2 - 1) \sin^{\pi/2}(\alpha_3 - 1)} \quad (5.6)$$

We are interested in the three-particle threshold generated by

$$\begin{aligned} \alpha_1 &= \alpha_2 = \alpha_3 = 1, \\ \lambda(t_4, t_1, t_2) &= \lambda(t, t_3, t_4) = 0. \end{aligned} \quad (5.7)$$

To isolate the discontinuity associated with the leading behavior we first extract the threshold factors

$$\mathcal{T}_3^{1/2} = \left[\frac{\lambda(t, t_3, t_4)}{t} \right]^{(j-n_3-n_4)/2} \times \left[\frac{\lambda(t_4, t_1, t_2)}{t_4} \right]^{(l_4-n_1-n_2)/2} \quad (5.8)$$

from each amplitude (leaving reduced amplitudes \tilde{G}) and absorb them in the definition of a full phase-space factor

$$\tilde{\Gamma}_{3(j,t)}^+ = \Gamma_{3(j,t)}^+ \mathcal{T}_3 \quad (5.9)$$

When the nonsense conditions $j = n_3 + n_4 - 1$ and $l_4 = n_4 = n_1 + n_2 - 1$ both hold, the threshold factors combine to give the right jacobian factors to change to transverse momentum variables. In addition to $t = q^2$ we write

$$\begin{aligned} t_1 &= k_1^2, \quad t_3 = k_3^2, \quad t_4 = k_4^2 = (q - k_3)^2, \\ t_2 &= k_2^2 = (k_4 - k_1)^2 = (q - k_3 - k_1)^2 \end{aligned} \quad (5.10)$$

In parallel with the discussion of the previous Section, we use the linear approximation for $\alpha(t)$ and absorb factors of α' in our definition of residue amplitudes. In analogy with (4.42) we can then write, close to the threshold,

$$\delta_t \left\{ \tilde{\Gamma}_{3(j,t)}^+ \right\} \equiv \delta_{q^2} \left\{ \tilde{\Gamma}_{3(q^2)}^+ \right\} = \delta_{q^2} \left\{ J_2(q^2) \right\} \quad (5.11)$$

where

$$J_2(q^2) = \frac{1}{(16\pi^3)^2} \int \frac{d^2k_1 d^2k_3}{k_1^2 k_3^2 (q - k_1 - k_3)^2} \quad (5.12)$$

There is a factor of ω^{-1} missing in (5.11) compared to (4.42) because we have already accounted for the presence of nonsense zeroes. The full (leading-behavior of the) three-particle discontinuity is

$$\delta_{q^2} \left\{ a^+(j, q^2) \right\} = \delta_{q^2} \left\{ J_2(q^2) \right\} \tilde{G}_{\tilde{\alpha}}(j, t^+) \tilde{G}_{\tilde{\alpha}}(j, t^-) \quad (5.13)$$

It is important to discuss why *two nonsense conditions hold*. The first condition, $j = n_3 + n_4 - 1$, holds because we will be considering the two reggeon nonsense state generating the two-reggeon cut. The second condition, $l_4 = n_4 = n_1 + n_2 - 1$, is more subtle. For the leading threshold behavior we set $n_r = \alpha_r = 1$, $r = 1, \dots, 3$. The second condition then becomes $n_4 = 1$ while the first condition becomes $j = n_4$. If we then consider $j \sim 1$ the second condition is satisfied. This argument actually demonstrates that the leading three-particle threshold contribution to the two-reggeon interaction, i.e. *the BFKL kernel, comes entirely from nonsense states*. For this argument we did not have to impose $q^2 \rightarrow 0$ even though the threshold is at $q^2 = 0$. Of course, the discussion of the previous Section also made clear that the simple transverse momentum integrals we have obtained are only a valid approximation for $j \sim 1$ and $q^2 \sim 0$.

We consider now the lowest order contributions to $\tilde{G}_{\tilde{\alpha}}(j, t^+)$ and $\tilde{G}_{\tilde{\alpha}}(j, t^-)$ (i.e. lowest order in g - the triple reggeon coupling). We consider the Regge poles at $n_4 = \alpha_4$ in $\tilde{G}_{\tilde{\alpha}}(j, t^+)$ and at $n_4 = \alpha_4^*$ in $\tilde{G}_{\tilde{\alpha}}(j, t^-)$. As illustrated in Fig. 5.2,

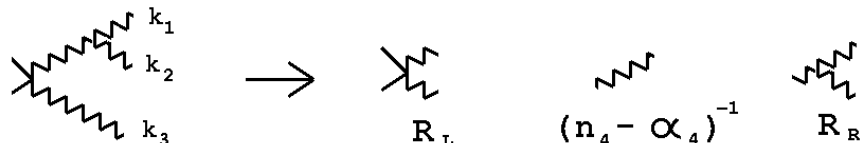


Fig. 5.2 Factorization of $\tilde{G}_{\tilde{\alpha}}(j, t^+)$

Regge pole factorization requires that we can write

$$\tilde{G}_{\tilde{\alpha}}(j, t^+) \sim \frac{R_L R_R}{n_4 - \alpha_4} \quad (5.14)$$

where R_L is the coupling of two reggeons to the external state (which we have taken to be two particles). For our purposes, we can take R_L to be a constant carrying zero color i.e.

$$R_L = \delta_{ij} \quad (5.15)$$

where i and j are color indices. R_R is the triple reggeon vertex, except that since we have extracted the nonsense zero there is no momentum factor. (This momentum factor would satisfy the relevant Ward identity constraint). Therefore we take

$$R_R = g c_{ijk} \quad (5.16)$$

Since we have already set $n_4 = (j - \alpha_3 + 1)$ we have $(n_4 - \alpha_4) = (\omega - \Delta_3 - \Delta_4)$ and so we can write

$$\tilde{G}_{\alpha}(j, t^+) = \frac{g c_{ijk}}{\omega - \Delta_3 - \Delta_4} \quad (5.17)$$

(although since we have already set $\alpha_3 = 1$ we could set $\Delta_3 = 0$). With the analogous expression for $\tilde{G}_{\alpha}(j, t^-)$ we obtain

$$\delta_{q^2} \left\{ a^+(j, q^2) \right\} = g^2 C_N \delta_{q^2} \left\{ J_2(q^2) \right\} \frac{1}{(\omega - \Delta_3 - \Delta_4)(\omega - \Delta_3^* - \Delta_4^*)} \quad (5.18)$$

$C_N = N$ is the color factor (for $SU(N)$) obtained by a simple application of Fig. 3.5(b), as illustrated in Fig. 5.3.

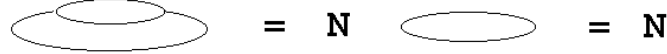


Fig. 5.3 The color factor C_N

Working to $O(g^2)$ in the overall discontinuity, we can neglect the $O(g^2)$ term in $\Delta(q^2)$. We then have

$$\delta_{q^2} \left\{ a^+(\omega, q^2) \right\} = \frac{g^2 N}{(16\pi^3)^2} \delta_{q^2} \left\{ \int \frac{d^2 k_1 d^2 k_3}{k_1^2 k_3^2 (q - k_1 - k_3)^2} \frac{1}{(\omega - \alpha' k_3^2 - \alpha' (q - k_3)^2)^2} \right\} \quad (5.19)$$

This is the discontinuity of the reggeon diagram shown in Fig. 5.4

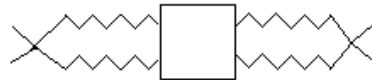


Fig. 5.4 A reggeon diagram

if we take the reggeon interaction to be

$$g^2 N K_1(k_3, q - k_3, k'_3, q - k'_3)$$

where $K_1(k_1, k_2, k_3, k_4)$ is given by (3.4), corresponding to the first transverse momentum diagram in Fig. 3.2. Clearly this disconnected interaction gives again the $O(g^2)$ reggeization that we already obtained in the previous Section. We have simply rederived this from the two reggeon state contained within the three reggeon state.

Note that since the two reggeon state includes particle poles (c.f. (2.3) and (4.34)) the absence of a pole in $k_4^2 = (q - k_3)^2$ in (5.18) implies that when we rewrite it as a reggeon diagram we include compensating factors in the interaction. This is equivalent to reinstating the nonsense zero momentum factor in R_R so that it becomes the full three reggeon vertex r_{ijk}^0 defined in the previous Section.

(5.18) is not the complete $O(g^2)$ contribution to the discontinuity. Since we sum over colors for each reggeon we can take (5.17), in which there is a Regge pole in the $t_4 = (k_1 + k_2)^2$ channel, to be the complete $O(g)$ contribution to $\tilde{G}_\alpha(j, t^+)$.

However, we must then allow for contributions to $\tilde{G}_\alpha(j, t^-)$ from Regge poles in the $t_{23} = (k_2 + k_3)^2$ and $t_{13} = (k_1 + k_3)^2$ channels. The reggeon amplitude with a pole in t_{23} is shown in Fig. 5.5.

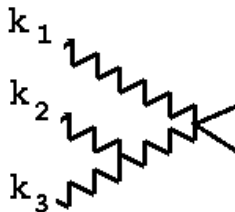


Fig. 5.5 A reggeon amplitude

In principle we should directly evaluate the contribution of this amplitude to the partial-waves that we have used up to this point. In general this would be a complicated transformation. However, as we now discuss, there are special kinematic situations in which the transformation simplifies.

The amplitude of Fig. 5.5 has a simple form in the partial-wave coupling scheme illustrated in Fig. 5.6. Let us compare, in general, the variables corresponding to Fig. 5.1 and Fig. 5.6.

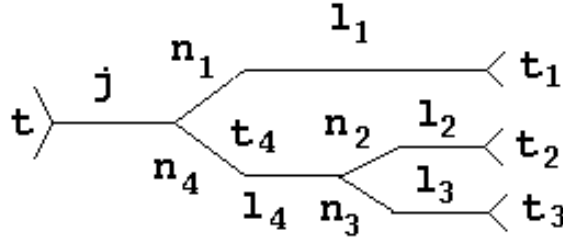


Fig. 5.6 Alternative coupling scheme

For Fig. 5.1 the angular variables conjugate to the angular momenta and helicities are defined[16] with respect to the plane in which the momenta of t and t_1 lie and the plane given by t_2 and t_3 . The variables of Fig. 5.6 are defined with respect to the plane of t and t_3 and that of t_2 and t_3 .

Consider now the leading threshold behavior at $t = q^2 = 0$. To obtain $q^2 = 0$ from three “massless” particles, i.e. with $k_i^2 = 0$, $i = 1,2,3$, *all three momenta must be parallel*. This implies that *in this special case* the relevant variables of Figs. 5.1 and 5.6 degenerate. The helicities of the three particles can be identified, the angles conjugate to j and n_4 can essentially be identified within each scheme and also in the two schemes. All singularities of the partial-wave amplitudes are associated with the threshold factors that we have already extracted. Consequently the reggeon amplitude of Fig. 5.6 can be simply expressed in terms of the variables of Fig. 5.1. That is we can write the contribution of the diagram of Fig. 5.5 to $\tilde{G}_\alpha(j, t^-)$ in the form

$$\tilde{G}_\alpha(j, t^-) \sim \frac{R_L R_R}{\omega - \Delta_1^* - \Delta_{23}^*} \quad (5.20)$$

where $\Delta_{23} = \alpha'(k_2 + k_3)^2$. Now we take $R_R = \delta_{ij}$ and R_L is the triple reggeon vertex. We have only to determine the relative sign, which we do by the following argument based on the antisymmetry properties of the two-reggeon state discussed earlier.

We need the relative contribution of the two reggeon diagrams shown in Fig. 5.7. From the analysis of the two-reggeon cut in the previous Section, we know that the reggeons forming the two reggeon state coupling to the particles must have opposite helicities. Since helicity is conserved by the reggeons in a reggeon diagram, the triple reggeon vertices in the two diagrams involve single reggeons of opposite helicity. That is one vertex is the parity transformation of the other and so must have the opposite sign (when all color labels are identical).

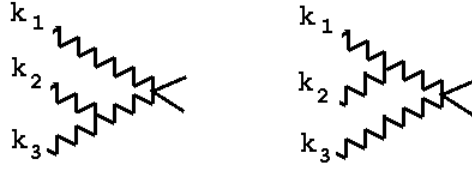


Fig. 5.7 Comparison of reggeon diagrams

We therefore take

$$R_L = -c_{ijk} \quad (5.21)$$

Inserting (5.17) and (5.20) in (5.13) we again obtain the discontinuity of a reggeon diagram of the form shown in Fig. 5.4 if we take the reggeon interaction to be

$$g^2 N K_2(k_3, q - k_3, k'_3, q - k'_3)$$

with $K_2(k_1, k_2, k_3, k_4)$ given by (3.4) and corresponding to the second diagram of Fig. 3.2 - apart from a factor of two which is obtained by adding the diagram with the pole in the t_{12} -channel. The color factor is obtained via the application of Fig. 3.5 illustrated in Fig. 5.8.

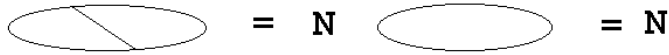


Fig. 5.8 Another color factor

Since we have determined both the overall magnitude and relative sign of K_1 and K_2 (the overall sign actually changes as we continue from timelike to spacelike q^2), the infra-red finiteness property of Section 3 has been obtained directly from unitarity. $K_1 + K_2$ is the complete kernel at $q^2 = 0$. K_3 vanishes at this point and since it has no discontinuity in q^2 can not be determined by unitarity. It is immediately determined as the first correction away from $q^2 = 0$ once we impose the Ward identity constraint (3.11) that is our input of gauge invariance. Therefore the full, conformally invariant, BFKL kernel is determined by the combination of t -channel unitarity and Ward identity constraints.

6. FOUR-REGGEON NONSENSE STATES

We now have all the apparatus in place to discuss the derivation, from the four-reggeon nonsense states, of the components of $K_{2,2}^{(4n)}$, the $O(g^4)$ kernel discussed

in [9]. We recall that $K_{2,2}^{(4n)}$ was defined by the sum of transverse momentum integrals

$$\frac{1}{(g^2 N)^2} K_{2,2}^{(4n)}(k_1, k_2, k_3, k_4) = K_0^{(4)} + K_1^{(4)} + K_2^{(4)} + K_3^{(4)} + K_4^{(4)}. \quad (6.1)$$

with

$$K_0^{(4)} = \sum k_1^4 k_2^4 J_1(k_1^2) J_1(k_2^2) (16\pi^3) \delta^2(k_2 - k_3), \quad (6.2)$$

$$K_1^{(4)} = -\frac{2}{3} \sum k_1^4 J_2(k_1^2) k_2^2 (16\pi^3) \delta^2(k_2 - k_3) \quad (6.3)$$

$$K_2^{(4)} = -\sum \left(\frac{k_1^2 J_1(k_1^2) k_2^2 k_3^2 + k_1^2 k_3^2 J_1(k_4^2) k_4^2}{(k_1 - k_4)^2} \right), \quad (6.4)$$

$$K_3^{(4)} = \sum k_2^2 k_4^2 J_1((k_1 - k_4)^2), \quad (6.5)$$

and

$$K_4^{(4)} = \frac{1}{2} \sum k_1^2 k_2^2 k_3^2 k_4^2 I(k_1, k_2, k_3, k_4), \quad (6.6)$$

The corresponding transverse momentum diagrams are shown in Fig. 6.1

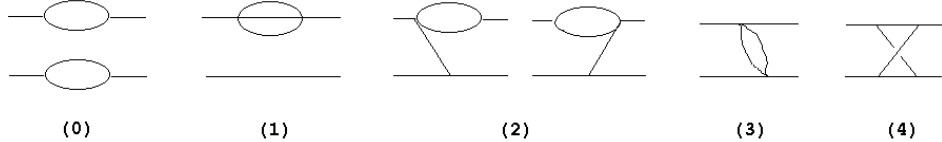


Fig. 6.1 (0), (1) - disconnected diagrams for the $O(g^4)$ kernel; (2), (3), (4) - connected diagrams.

We will encounter essentially all of the subtleties of multiparticle multi-Regge theory in this Section and although we will try to give a coherent self-contained discussion it is likely that [16] is an essential reference to follow the full details. We use the partial-wave coupling scheme shown in Fig. 6.2.

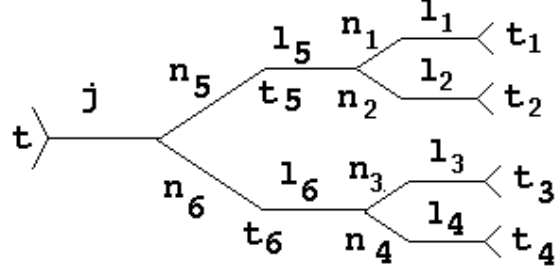


Fig. 6.2 Coupling scheme for the eight-particle state

The partial-wave projection of the unitarity integral is

$$a_j(t) - a_j^i(t) = \int d\rho \sum_{|n_5+n_6| \leq j} \sum_{|n_1+n_2| \leq l_5} \sum_{|n_3+n_4| \leq l_6} \sum_{r=1}^6 \sum_{l_r \geq |n_r|} a_{j \tilde{l} \tilde{n}}(t, \tilde{t}) a_{j \tilde{l} \tilde{n}}^i(t, \tilde{t}) \quad (6.7)$$

where now the i denotes amplitudes evaluated below the eight-particle cut.

As before, we consider even signature in j , and keep the terms with $l_r = n_r$, $r = 1, \dots, 6$. The helicity integrals giving the continuation to complex j of the sums in (6.7) are (keeping only odd signature in the n_r)

$$\begin{aligned} & \frac{1}{2^{12}} \sin \frac{\pi}{2} j \int \frac{dn_5 dn_6}{\sin \frac{\pi}{2} (j - n_5 - n_6)} \\ & \int \frac{dn_1 dn_2}{\sin \frac{\pi}{2} (n_5 - n_1 - n_2 + 1) \sin \frac{\pi}{2} (n_1 - 1) \sin \frac{\pi}{2} (n_2 - 1)} \\ & \int \frac{dn_1 dn_2}{\sin \frac{\pi}{2} (n_6 - n_3 - n_4 + 1) \sin \frac{\pi}{2} (n_3 - 1) \sin \frac{\pi}{2} (n_4 - 1)} \end{aligned} \quad (6.8)$$

This time the structure of both the n_1 and n_2 integrations and the n_3 and n_4 integrations is the same as for Γ^- in (4.24). Correspondingly nonsense zeroes (at the nonsense points we discuss below) ensure that no internal two-reggeon cuts are generated that would lead to a four-reggeon cut. As we discussed in the last Section, this zero can be identified with the zero of the triple reggeon vertex. The threshold we consider is produced by the Regge poles at $l_r = \alpha_r = \alpha(t_r)$, $r = 1, \dots, 4$. The two-reggeon cut is produced by Regge poles at $l_5 = \alpha_5$ and $l_6 = \alpha_6$, together with the nonsense pole at $j = n_5 + n_6 - 1$.

We use the Regge poles to perform the helicity integrals over n_1, n_2, n_3 and n_4 in (6.8) and, as usual, use two-particle unitarity to eliminate the phase-space integrations for the two particle states to which the $\alpha_1, \alpha_2, \alpha_3$ and α_4 Regge poles couple. Retaining for the moment the integrations over n_5 and n_6 and extracting nonsense factors we obtain, for $j \sim 1$,

$$\begin{aligned} \Gamma_{4[j,t]}^+ \sim & \frac{\pi^4}{2^6} \int \frac{dn_5 dn_6}{(j - n_5 - n_6 + 1)} \\ & \int d\tilde{\rho} \frac{1}{\sin^{\frac{\pi}{2}}(\alpha_1 - 1) \sin^{\frac{\pi}{2}}(\alpha_2 - 1) \sin^{\frac{\pi}{2}}(\alpha_3 - 1) \sin^{\frac{\pi}{2}}(\alpha_4 - 1)} \end{aligned} \quad (6.9)$$

where $\int d\tilde{\rho}$ is a product of integrations of the form of (4.22) i.e.

$$\begin{aligned} \int d\tilde{\rho}(t, t_1, \dots, t_6) = & \int_{\lambda(t, t_5, t_6) > 0} d\tilde{\rho}(t, t_5, t_6) \\ & \int_{\lambda(t_5, t_1, t_2) > 0} d\tilde{\rho}(t_5, t_1, t_2) \int_{\lambda(t_6, t_3, t_4) > 0} d\tilde{\rho}(t_6, t_3, t_4) \end{aligned} \quad (6.10)$$

The boundaries of the integration region that matter for us are those we have shown. $\lambda(t, t_5, t_6) = 0$ is involved in both the two-reggeon cut and the four-particle threshold. $\lambda(t_5, t_1, t_2) = 0$ and $\lambda(t_6, t_3, t_4) = 0$ will contribute to the four-particle threshold.

We are, of course, interested in studying the four-particle threshold in combination with the two-reggeon cut. If the phase-space (6.10) is to reduce to transverse momentum integrals then, in addition to the nonsense condition imposed by the two-reggeon cut, nonsense conditions must be satisfied at the two “internal vertices” i.e. we must have

$$l_5 = n_5 \sim n_1 + n_2 - 1 , \quad l_6 = n_6 \sim n_3 + n_4 - 1 , \quad (6.11)$$

Extracting the leading threshold behavior will set $n_1 = n_2 = n_3 = n_4 = 1$ and so (6.11) will be satisfied if $n_5 \sim n_6 \sim 1$. If we consider $t \sim 0$ then the two-reggeon cut is generated at $t_5 \sim t_6 \sim t/4$ which, provided the reggeon slope α' is finite, implies also that $n_5 \sim n_6 \sim 1$, as we require. Therefore, if α' is finite and we are interested strictly in the two-reggeon cut, $j \sim 1$ is equivalent to

$$t \sim t_5 \sim t_6 \sim (j - 1)/\alpha' \sim 0 . \quad (6.12)$$

It follows that, for $\alpha' \neq 0$, the leading four-particle threshold contribution to the two-reggeon interaction, in the neighborhood of $j = 1$, is indeed given by transverse

momentum integrals. However, we are interested in the limit $\alpha' \rightarrow 0$, which in principle allows t, t_5, t_6 to be arbitrarily large while satisfying (6.12). Nevertheless we shall find that there are additional kinematic arguments that lead us to impose $t_5 \sim t_6 \sim 0$, in addition to $t \sim 0$ and $j \sim 1$. In this case the nonsense conditions remain valid as $\alpha' \rightarrow 0$. Clearly we will obtain only an infra-red approximation to the reggeon interaction we are looking for.

Extracting threshold behavior \mathcal{T}_4 in analogy with (5.8) and defining a full phase-space factor

$$\tilde{\Gamma}_{4(j,t)}^+ = \Gamma_{4(j,t)}^+ \mathcal{T}_4 \quad (6.13)$$

we can write, in parallel with the discussion of previous Sections, except that we still retain the integrations over n_5 and n_6 ,

$$\begin{aligned} \delta_t \left\{ \tilde{\Gamma}_{4(j,t)}^+ \right\} &\equiv \delta_{q^2} \left\{ \tilde{\Gamma}_{4(q^2)}^+ \right\} \\ &= \delta_{q^2} \left\{ J_3(q^2) \left[\frac{\pi^4}{2^6} \int \frac{dn_5 dn_6}{(j - n_5 - n_6 + 1)} \right] \right\} \end{aligned} \quad (6.14)$$

where

$$J_3(q^2) \left[\dots \right] = \frac{1}{(16\pi^3)^3} \int \frac{d^2 k_1 d^2 k_3 d^2 k_4}{k_1^2 k_3^2 k_4^2 (q - k_1 - k_3 - k_4)^2} \left[\dots \right] \quad (6.15)$$

The transverse momenta are now defined by

$$\begin{aligned} t_i &= k_i^2 \quad i = 1, \dots, 6 \\ k_2 &= q - k_1 - k_3 - k_4 \\ k_5 &= k_1 + k_2 \\ k_6 &= k_3 + k_4 \end{aligned} \quad (6.16)$$

The leading-behavior of the four-particle discontinuity is then, formally,

$$\delta_{q^2} \left\{ a^+(j, q^2) \right\} = \delta_{q^2} \left\{ J_3(q^2) \left[\frac{\pi^4}{2^6} \int \frac{dn_5 dn_6 \tilde{G}_\alpha(j, t^+) \tilde{G}_\alpha(j, t^-)}{(j - n_5 - n_6 + 1)} \right] \right\} \quad (6.17)$$

where $\tilde{G}_\alpha(j, t)$ is now a two-particle/four-reggeon amplitude.

At first sight $K_0^{(4)}$ is the simplest to derive. It is certainly the simplest to discuss. Since it is a sum of diagrams of the form of Fig. 6.1(0), it should be generated by

a diagonal product of partial-wave amplitudes as a straightforward generalization of the discussion of K_1 in the BFKL kernel. Instead of Fig. 5.2, we have the factorization illustrated in Fig. 6.3

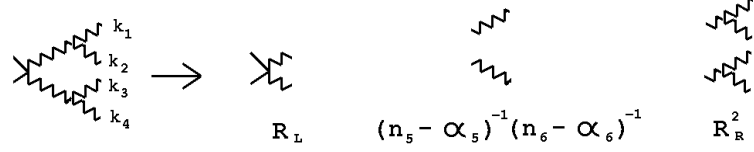


Fig. 6.3 Factorization of $\tilde{G}_\alpha(j, t^+)$

that is we write

$$\tilde{G}_\alpha(j, t^+) \sim \frac{R_L R_R^2}{(n_5 - \alpha_5)(n_6 - \alpha_6)} \quad (6.18)$$

where R_R is the triple Regge vertex. The contribution from $\tilde{G}_\alpha(j, t^-)$ is analogous.

However, the poles at $n_5 = \alpha_5$ and $n_6 = \alpha_6$ together with the complex conjugate poles in $\tilde{G}_\alpha(j, t^-)$, give for the helicity integral in (6.17)

$$\int \frac{dn_5 dn_6}{(j - n_5 - n_6 + 1)(n_5 - \alpha_5)(n_6 - \alpha_6)(n_5 - \alpha_5^*)(n_6 - \alpha_6^*)} \quad (6.19)$$

Using $(j - n_5 - n_6 + 1)^{-1}$ for one integration, gives

$$\begin{aligned} & \frac{1}{(\alpha_6 - \alpha_6^*)} \left(\frac{1}{(j - \alpha_5 - \alpha_6 + 1)(j - \alpha_5^* - \alpha_6 + 1)} \right. \\ & \left. - \frac{1}{(j - \alpha_5 - \alpha_6^* + 1)(j - \alpha_5^* - \alpha_6^* + 1)} \right) \end{aligned} \quad (6.20)$$

Since two reggeon propagators appear in each term we could, after insertion back in (6.17), extract the residue of one term as (the discontinuity of) a reggeon interaction. (We would get the same result from either term since we would make the approximation $\alpha_5 = \alpha_5^*$ and identify the first term with $a_j(t^+)$ and the second with $a_j(t^-)$). However, we do not obtain $K_0^{(4)}$. The additional factor of $(\alpha_6 - \alpha_6^*)^{-1}$ in (6.20) has the effect of removing the corresponding J_1 factor in Fig. 6.1(0). Consequently we

do not produce $K_0^{(4)}$, but again reproduce the lowest-order reggeization K_1 . (There is not actually a pole at $\alpha_6 = \alpha_6^*$ since the two terms in (6.20) cancel at this point.)

It should be no surprise that $K_0^{(4)}$ is not generated via a scale-invariant unitarity analysis. It has no interpretation as a trajectory function contribution and as a reggeon diagram it is completely dependent on the existence of a rapidity-gap minimum cut-off which defines the “finite rapidity interval” within which the two bubble interactions of $K_0^{(4)}$ can occur. If this cut-off is set to zero, as effectively is done in the above unitarity analysis, the diagram disappears.

The situation is different for the next contribution we discuss. We consider $K_4^{(4)}$, corresponding to the diagram of Fig. 6.1(4). This is an off-diagonal product of the same reggeon diagrams that at first sight produce $K_0^{(4)}$. To discuss this we need, in principle, to obtain an expression for the reggeon diagram of Fig. 6.4 in the partial-wave coupling scheme of Fig. 6.2.

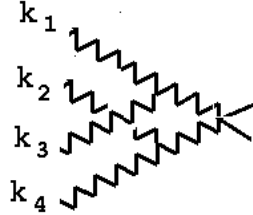


Fig. 6.4 A reggeon contribution to $\tilde{G}_\alpha(j, t^-)$.

As in our discussion of Fig. 5.5 in the last Section, a complicated transformation is involved in general. We can again impose special kinematic restrictions to simplify the situation.

If we impose *both* $t = (k_1 + k_2 + k_3 + k_4)^2 = 0$ and, say, $(k_1 + k_3)^2 = 0$ on four massless particles (allowing the k_i to be four momenta) then, necessarily, *all the momenta are parallel*. Therefore the angular variables of Fig. 6.2 and the coupling scheme associated with Fig. 6.4 degenerate. (All the λ -functions in (6.10) vanish and the divergences of the partial-wave amplitudes are again extracted by the threshold factors involved in changing to transverse momenta.) However, there is a further problem not present in our discussion of Fig. 5.5. In the reggeon diagram of Fig. 6.4, the variables $(k_1 + k_3)^2$ and $(k_2 + k_4)^2$ are clearly transverse momenta and also are zero when all the momenta are parallel. In terms of the variables associated with the coupling scheme of Fig. 6.2, these “transverse momentum variables” are expressed

in terms of angular variables that are the analogue of rapidity variables in the s -channel. Consequently taking $(k_1 + k_3)^2 \sim 0$ and $(k_2 + k_4)^2 \sim 0$ limits the angular range (the relative rapidity of the (t_5, t_1, t_2) and (t_6, t_3, t_4) vertices) integrated over when projecting Fig. 6.4 onto the partial-waves of Fig. 6.2. This range determines the normalization of the contribution of Fig. 6.4. Thus defining the transverse momentum scale implied by writing

$$t = (k_1 + k_2 + k_3 + k_4)^2 \sim 0 , \quad t_{13} = (k_1 + k_3)^2 \sim 0 \quad (6.21)$$

translates into a rapidity cut-off on the relative rapidity of the (t_5, t_1, t_2) and (t_6, t_3, t_4) vertices that determines the overall normalization when we combine the reggeon diagram of Fig. 6.4 with that of Fig. 6.3.

When (6.21) is satisfied we can write

$$\tilde{G}_\alpha(j, t^-) \sim \tilde{C} \frac{R_L^2 R_R}{(n_5 + n_6 - \alpha_{13}^* - \alpha_{24}^*)} \quad (6.22)$$

where R_L is the triple Regge vertex, $\alpha_{ij} = \alpha((k_i + k_j)^2)$, and \tilde{C} depends on the transverse momentum scale. Combining (6.22) with (6.18) and inserting in (6.17) we obtain, instead of the helicity integral (6.19),

$$\begin{aligned} & \int \frac{dn_5 dn_6}{(j - n_5 - n_6 + 1)(n_5 - \alpha_{12})(n_6 - \alpha_{34})(n_5 + n_6 - \alpha_{13}^* - \alpha_{24}^*)} \\ & \rightarrow \frac{1}{(j - \alpha_{12} - \alpha_{34} + 1)(j - \alpha_{13}^* - \alpha_{24}^* + 1)} \end{aligned} \quad (6.23)$$

Returning to (6.17) we obtain

$$\delta_{q^2} \left\{ a^+(j, q^2) \right\} \sim \frac{g^4 N^2}{2} \delta_{q^2} \left\{ J_3(q^2) \left[\frac{1}{(j - \alpha_{12} - \alpha_{34} + 1)(j - \alpha_{13}^* - \alpha_{24}^* + 1)} \right] \right\} \quad (6.24)$$

where the color factor $N^2/2$ is obtained from Fig. 6.5.

$$\text{Diagram: } \text{A box diagram with four external lines. The top and bottom lines are horizontal, and the left and right lines are vertical. The top-left and bottom-right corners are connected by a diagonal line. The top-right and bottom-left corners are connected by a diagonal line. This forms a box with an 'X' inside.} \equiv \frac{N}{2} \text{Diagram: } \text{A circle divided into four quadrants by a vertical and a horizontal line. The top-right quadrant is shaded.} = \frac{N^2}{2} \text{Diagram: } \text{A circle with no internal lines or shading.} = \frac{N^2}{2}$$

Fig. 6.5 Color factor for the box diagram.

Clearly (6.24) is the four-particle discontinuity of the reggeon diagram Fig. 5.4 with $K_4^{(4)}$ as the reggeon interaction.

There are some important general points related to this last derivation which we postpone discussion of until after we have discussed the remaining terms in $K_{2,2}^{(4)}$. These involve reggeon diagrams of the form of Fig. 6.6 that contain 1-3 reggeon interactions, either via an intermediate reggeon or as a direct coupling, and are naturally defined in the coupling scheme of Fig. 6.7.

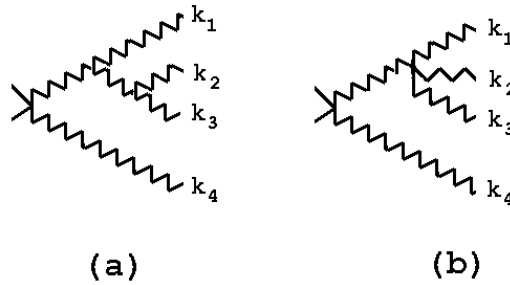


Fig. 6.6 (a) 1-3 reggeon interaction via an intermediate reggeon (b) an elementary 1-3 reggeon interaction.

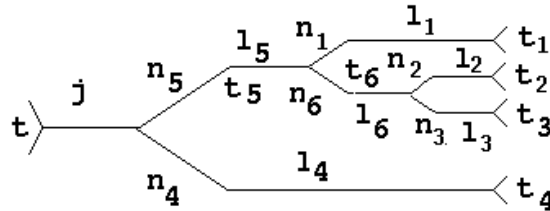


Fig. 6.7 Alternative coupling scheme

A nonsense zero will automatically prevent the intermediate reggeon in Fig. 6.6(a) from participating in a Regge cut. The Ward identity constraints then determine that this diagram gives a 1-3 reggeon interaction of the form

$$r_{13}(k_1, k_2, k_3) \sim \frac{k_1 \cdot (k_2 + k_3) k_2 \cdot k_3}{(k_2 + k_3)^2} \quad (6.25)$$

However, in the limit $k_1^2, k_2^2, k_3^2 \rightarrow 0$ this reduces to $k_1 \cdot k_2 + k_1 \cdot k_3$ and summing over such terms we simply obtain

$$r_{13}(k_1, k_2, k_3) \sim (k_1 + k_2 + k_3)^2 = k^2. \quad (6.26)$$

Therefore for the purpose of studying threshold contributions it suffices to take $r_{13} \sim k^2$, as in Fig. 6.1(1), (2) and (3). In this case the diagram of Fig. 6.6(a) should not be distinguished from that of Fig. 6.6(b).

To obtain the diagrams of Fig. 6.1(2) we need to consider the product of a diagram of the form of Fig. 6.3 with the conjugate of Fig. 6.6(b). Again the transformation from the coupling scheme of Fig. 6.7 to that of Fig. 6.2 is simple only if we impose an additional kinematic constraint, such as $(k_1 + k_2 + k_3)^2 \sim 0$, which requires that all the momenta participating in the threshold are (close to) parallel. This constraint also leads to an uncertainty in the overall normalization. However, after it is imposed, it is straightforward to essentially repeat (6.22) - (6.24) and obtain the first diagram of Fig. 6.1(2) as the reggeon interaction. The second diagram is obviously obtained by the conjugate analysis.

Fig. 6.1(1) is a product of diagrams of the form of Fig. 6.6(b). Since these diagrams are described by the same partial-wave it is, at first sight, simple to derive as an immediate generalization of (5.14)-(5.19). Similarly Fig. 6.1(3) is a non-diagonal product of diagrams of the form of Fig. 6.6(b). As a result, the derivation is an immediate generalization of that of K_2 in Section 5. There are, however, some important qualifications that we must make. The 1-3 reggeon coupling appearing in Fig. 6.6(b) can be generated by intermediate t -channel states that are not nonsense states. Consequently we can not argue immediately that the integrals appearing in Figs. 6.1(2) and (4) are transverse momentum integrals. The following discussion shows, nevertheless that if these diagrams appear at all in the scale-invariant approximation then a transverse momentum integral must be an infra-red approximation.

Because Fig. 6.1(2) involves the reggeon diagram of Fig. 6.3, its' derivation is complete (for $q^2 = 0$) for the leading threshold behavior given by the “bubble diagram”, which is then necessarily a transverse momentum diagram. As we have discussed in [9], the 1-3 reggeon coupling appearing in Figs. 6.1(1), (2) and (3) is determined by a Ward identity constraint involving Figs. 6.1(2) and (3). This constraint is illustrated in Fig. 6.8 (a dashed line indicates zero transverse momentum)

$$- \text{ } \begin{array}{c} \text{---} \\ \text{---} \end{array} \text{ } \text{---} \text{ } + \text{ } \begin{array}{c} \text{---} \\ \text{---} \end{array} \text{ } \text{---} \text{ } = \text{ } 0$$

Fig. 6.8 The Ward identity constraint for K^{4n} .

and has the form

$$r_{13}^2 \sim r_{13} r_{ijk} \quad (6.27)$$

giving both zero and non-zero solutions for r_{13} . If we assume the non-zero solution is the correct one, then this constraint implies that Fig. 6.1(3) must be present, in addition to Fig. 6.1(2), as a transverse momentum diagram. Infra-red finiteness is then satisfied provided the full box diagram of Fig. 6.1(4) is present. (That is the part of the box diagram containing thresholds in $(k_1 - k_3)^2$ and $(k_1 - k_4)^2$, which are not accessible within the t -channel unitarity integral must also be present.) The presence of Fig. 6.1(1), which can not be distinguished[9] from Fig. 6.1(0) in the forward direction, is then required by infra-red finiteness of the kernel after integration[7, 9].

It is clear that in discussing the diagrams of Fig. 6.1 we have had, in each case, to impose a leading threshold behavior constraint *in addition to imposing* $q^2 \rightarrow 0$. This means that our discussion is restricted to the forward kernel and to the leading infra-red behaviour in the additional transverse momentum variables, producing related uncertainties in overall normalization. In particular, the derivation of $K_4^{(4)}$ applies to the leading threshold behavior as $(k_1 + k_3)^2 \rightarrow 0$ and by analogy the leading behavior when $(k_2 + k_4)^2 \rightarrow 0$, $(k_1 + k_2)^2 \rightarrow 0$ and $(k_3 + k_4)^2 \rightarrow 0$. In [9] we argued that at $q^2 = 0$, these thresholds can be extracted from the box diagram and we can write

$$K_{2,2}^{(4n)} = (K_{BFKL}/2)^2 + \mathcal{K}_2 \quad (6.28)$$

where \mathcal{K}_2 contains the thresholds and is a separate infra-red finite kernel. We also derived the eigenvalue spectrum of \mathcal{K}_2 and showed that it satisfies the crucial property of *holomorphic factorization*.

The analysis of this Section can be summarized as showing that the forward kernel does indeed contain the two terms present in (6.28) but we can not determine their relative normalization. The fundamental new result is clearly that the \mathcal{K}_2 component can be unambiguously derived from unitarity. The infra-red finiteness and Ward identity constraints imply that all the remaining parts of $K_{2,2}^{(4n)}$ can be uniquely written as $(K_{BFKL})^2$. There is also a further very important property which distinguishes \mathcal{K}_2 from To properly explain this requires the full asymptotic dispersion theory of [16]. We can briefly summarize the essential point as follows.

As elaborated in [16], the different multiple discontinuities of a multiparticle amplitude have different continuations to complex angular momenta and helicities. We can embed $K_4^{(4)}$, as a reggeon interaction, in an eight-point amplitude as illustrated

in Figs. 6.9 and 6.10. There are then two classes of multiple discontinuities that have to be considered in defining the j -plane continuations that we have utilised. An example of the first class is illustrated in Fig. 6.9.

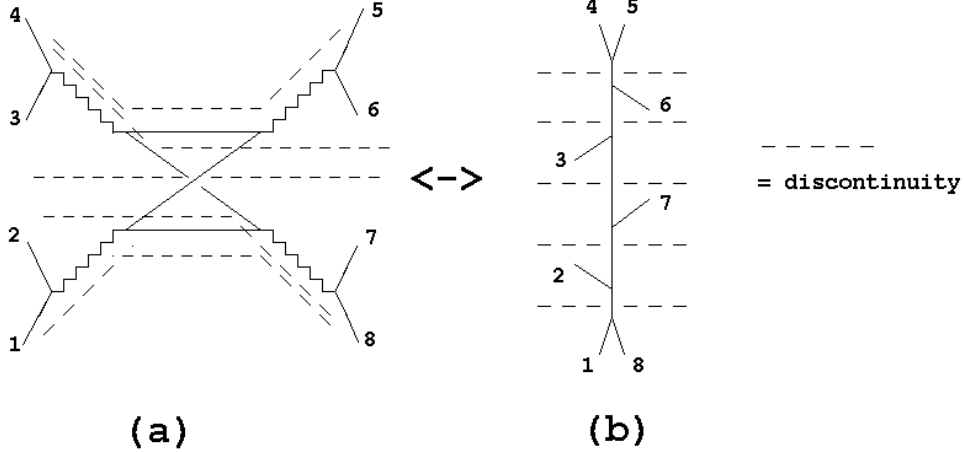


Fig. 6.9 (a) Multiple discontinuities of the eight-point amplitude (b) the corresponding tree graph.

Other examples in the same class would interchange the reggeons relative to the discontinuities taken. An example of the second class is illustrated in Fig. 6.10.

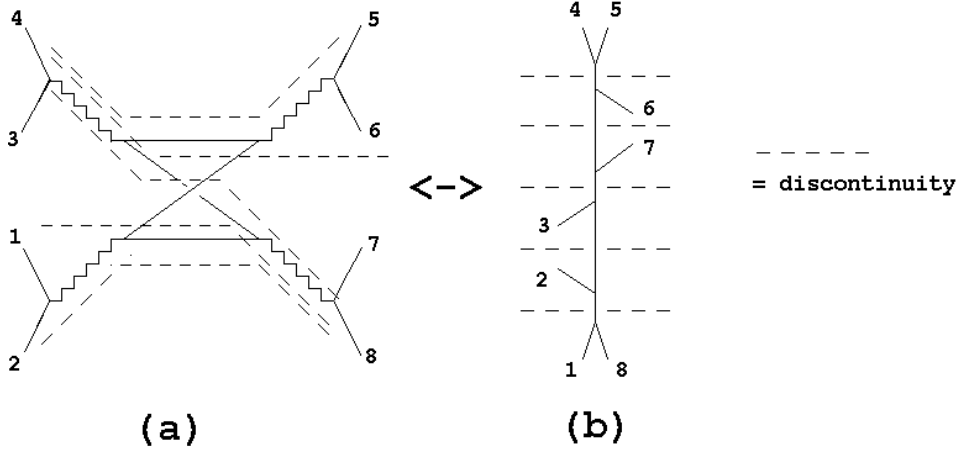


Fig. 6.9 (a) Alternative discontinuities of the eight-point amplitude (b) the corresponding tree graph

As in the examples we have shown, the two classes of multiple discontinuities differ in general only by one discontinuity. Fig. 6.9 contains the s_{3456} discontinuity,

whereas Fig. 6.10 contains instead the s_{4567} discontinuity. The s_{3456} discontinuity necessarily involves also taking a discontinuity of the box diagram (of the $(k_1 - k_3)^2$ form) whereas the s_{4567} discontinuity does not. All the connected diagrams of $(K_{BFKL})^2$ contain the necessary discontinuity (as do those of the leading-order K_{BFKL} .) On the other hand, the thresholds of \mathcal{K}_2 are compatible only with the s_{4567} discontinuity. It follows that the two terms in (6.28) will be separated by the process of taking the multiple discontinuities. $(K_{BFKL})^2$ will appear in Fig. 6.9 whereas \mathcal{K}_2 will appear in Fig. 6.10.

We use the partial-wave projection of Fig. 4.3 and consider the continuation to complex j , n_1 , n_2 n'_1 , n'_2 . Corresponding to their distinction with respect to one discontinuity, the multiple discontinuities of Figs. 6.9 and 6.10 differ in one feature of the analytic continuations made. For example, in both cases a continuation is made from

$$n_2 > 0, \quad n'_1 > 0, \quad n'_2 > n_2, \quad n_1 + n_2 > n'_1 + n'_2 \quad (6.29)$$

whereas, for Fig. 6.9 the final continuation is made from

$$j > n_1 + n_2 \quad (6.30)$$

while for Fig. 6.10 it is made from

$$j < n_1 + n'_2 \quad (6.31)$$

As a result a distinct analytically continued amplitude is defined in each case.

Although both partial-wave amplitudes appear similarly in the BFKL kernel, they are distinguished in the more general framework of multi-Regge theory. Since K_{BFKL} contributes only to Fig. 6.9, it follows that the separation in (6.28) distinguishes a leading-order contribution to a new partial-wave amplitude, i.e. \mathcal{K}_2 , from a non-leading contribution to the partial-wave amplitude that also contains the leading-order kernel. Not surprisingly the non-leading contribution suffers most from scale ambiguities.

7. CONCLUSIONS

We have demonstrated that the direct analysis of t -channel unitarity is able to give a firm foundation to the results of [7]. Not surprisingly the limitations of the results are also apparent. These include uncertainties in normalization due to

scale-dependence and infra-red kinematical constraints. Our non-leading results are essentially summarized by writing for the full BFKL kernel $K_{2,2}(q, k, k')$

$$K_{2,2}(q, k, k') \xrightarrow{q^2, k^2, k'^2 \rightarrow 0} g^2 K_{BFKL} + O(g^4)(K_{BFKL})^2 + O(g^4)\mathcal{K}_2 \quad (7.1)$$

indicating that both the overall normalization and the normalization of \mathcal{K}_2 relative to $(K_{BFKL})^2$ are not determined. Results obtained by Kirschner[11] from the multi-Regge effective lagrangian are completely consistent with (6.1), although the separate significance of \mathcal{K}_2 is not apparent in the s -channel formalism. A fundamental new result obtained in this paper is that \mathcal{K}_2 can be unambiguously derived from t -channel unitarity as the leading-order contribution of a new (analytically continued) multi-particle partial-wave amplitude. We had previously identified \mathcal{K}_2 only as a separately infra-red finite component of the kernel. The holomorphic factorization properties of its' spectrum are strongly suggestive that the full (non-forward) leading-order form of this amplitude will be conformally invariant. Indeed in a separate paper[10] we have constructed a candidate for this amplitude using the Ward identity constraints.

It is clear that if a reggeon interaction is unambiguously derivable from t -channel unitarity, it will necessarily be scale-invariant and presumably must be the leading-order infra-red approximation to some well-defined partial-wave amplitude. The extrapolation away from the infra-red region will then satisfy Ward identity constraints which, we conjecture, necessarily lead to conformal invariance. From the multi-Regge theory of [16] we know there exists a vast array of distinct partial-wave amplitudes describing Regge limits of dispersion-relation defined components of multiparticle amplitudes. The BFKL kernel, the triple Regge kernel[22, 7], and the new \mathcal{K}_2 kernel we have derived are amongst the simplest examples. Our results and those of [28], when added to previous results on the BFKL kernel, are consistent with the conjecture that all such amplitudes have a leading-order conformally invariant approximation. The physical significance of this approximation remains to be determined.

In [29] we have also outlined a program whereby the scale-dependence of non-leading reggeon amplitudes might be studied via the Ward identity constraints. We leave to a future study the possibility that the formalism of this paper can be extended in this direction.

Acknowledgements

We are grateful to J. Bartels, R. Kirschner and L. Lipatov for valuable discussions of this work.

References

- [1] A. R. White, *Int. J. Mod. Phys. A***8**, 4755 (1993).
- [2] A. R. White, *Phys Rev D***29**, 1435 (1984).
- [3] E. A. Kuraev, L. N. Lipatov, V. S. Fadin, *Sov. Phys. JETP* **45**, 199 (1977) ; Ya. Ya. Balitsky and L. N. Lipatov, *Sov. J. Nucl. Phys.* **28**, 822 (1978); L. N. Lipatov, in *Perturbative QCD*, ed. A. H. Mueller (World Scientific, 1989).
- [4] R. Kirschner, L. N. Lipatov and L. Szymanowski, *Nucl. Phys.* **B425**, 579 (1994), *Phys. Rev.* **D51**, 838 (1995).
- [5] L. N. Lipatov, DESY 95-029, hep-ph/9502308.
- [6] H. Cheng and C. Y. Lo, *Phys. Rev.* **D13**, 1131 (1976) and **D15**, 2959 (1977).
- [7] A. R. White, *Phys. Lett.* **B334**, 87 (1994).
- [8] V. S. Fadin and L. N. Lipatov, *Nucl. Phys.* **B406**, 259 (1993); J. Bartels, **DESY preprint**, DESY 91-074 (1991) and *Zeitsch. Phys.* **C60**, 471 (1993).
- [9] C. Corianò and A. R. White *Phys. Rev. Lett.* **74**, 4980 (1995), *Nucl. Phys.* **B451**, 231 (1995).
- [10] C. Corianò, R. R. Parwani and A. R. White, ANL-HEP-PR-95-53/IFTIP-BBSR-95-80/UF-IFT-HEP-95-20.
- [11] R. Kirschner, LEIPZIG-18-1995, hep-ph/9505421.
- [12] B. M. McCoy and T. T. Wu, *Phys. Rev.* **D13**, 369, 379, 424, 484, 508 (1976).
- [13] V. N. Gribov, *Soviet Phys. JETP* **26**, 414 (1968)
- [14] V. N. Gribov, I. Ya. Pomeranchuk and K. A. Ter-Martirosyan, *Phys. Rev.* **139B**, 184 (1965).
- [15] S. Mandelstam, *Nuovo Cimento* **30** 1113, 1127, 1143 (1963).
- [16] A. R. White, *Int. J. Mod. Phys. A***6**, 1859 (1990).
- [17] H. P. Stapp and A. R. White, *Phys. Rev. D***26**, 2145 (1982).

- [18] H. P. Stapp, in *Structural Analysis of Collision Amplitudes*, proceedings of the Les Houches Institute, eds. R. Balian and D. Iagolnitzer (North-Holland 1976).
- [19] A. A. Migdal, A. M. Polyakov and K. A. Ter-Martirosyan, *Zh. Eksp. Teor. Fiz.* **67**, 84 (1974); H. D. I. Abarbanel and J. B. Bronzan, *Phys. Rev.* **D9**, 2397 (1974).
- [20] M. T. Grisaru, H. J. Schnitzer and H-S. Tsao, *Phys. Rev.* **8**, 4498 (1973).
- [21] J. B. Bronzan and R. L. Sugar, *Phys. Rev.* **D17**, 585 (1978); J. Bartels, *Nucl. Phys.* **B151**, 293 (1979), **B175**, 365 (1980)
- [22] J. Bartels and M. Wüsthoff, *Z. Phys.* **C66**, 157 (1995).
- [23] G. 't Hooft, *Nucl. Phys.* **B33**, 173 (1971).
- [24] C. Y. Lo, *Phys. Rev.* **D23**, 508 (1981).
- [25] Yu. A. Simonov, *Sov. Phys. JETP* **21**, 160 (1965).
- [26] D. I. Olive and J. C. Polkinghorne, *Phys. Rev.* **171**, 1475 (1968).
- [27] A. R. White, *Phys. Rev.* **D10**, 1236 (1974).
- [28] J. Bartels, L. N. Lipatov and M. Wüsthoff, hep-ph/9509303.
- [29] C. Corianò and A. R. White ANL-HEP-CP-94-79, Proceedings of the XXIV International Symposium on Multiparticle Dynamics, Vietri sul Mare, Italy (1994).